

copy!

THE ROLE OF TIDAL MIXING IN
RUPERT AND HOLBERG INLETS

by

KENNETH FRANCIS DRINKWATER
B.Sc., University of Calgary, 1970

A THESIS SUBMITTED IN PARTIAL FULFILMENT OF
THE REQUIREMENTS FOR THE DEGREE OF
MASTER OF SCIENCE

in the Department
of
Physics
and the Institute of Oceanography

We accept this thesis as conforming to the
required standard.

THE UNIVERSITY OF BRITISH COLUMBIA

April, 1973

In presenting this thesis in partial fulfilment of the requirements for an advanced degree at the University of British Columbia, I agree that the Library shall make it freely available for reference and study.

I further agree that permission for extensive copying of this thesis for scholarly purposes may be granted by the Head of my Department or by his representatives. It is understood that copying or publication of this thesis for financial gain shall not be allowed without my written permission.

Department of PHYSICS (OCEANOGRAPHY)

The University of British Columbia
Vancouver 8, Canada

Date MAY 1, 1973

ABSTRACT

Analysis of monthly observations of temperature, salinity and dissolved oxygen content in the basin formed by Rupert and Holberg Inlets reveals a greater degree of mixing than that found in most British Columbia Inlets. Although relatively uniform water properties are constantly found, there are large monthly variations of the actual values.

The water temperature correlates with the solar radiation while the salinity changes follow the river runoff which is in turn controlled by precipitation. The variation in dissolved oxygen content appears due to a combination of biological influences and influx of Pacific Oceanic water.

A model has been developed which ascribes the monthly fluctuations and vertical homogeneity to an accumulation of irregular mixing events associated with the tidal flow through Quatsino Narrows, a shallow connecting channel.

Thermal microstructure measurements disclose a region of deep turbulent mixing near the narrows and provide evidence of an up-inlet flow beneath the thermocline in Rupert and Holberg Inlets.

TABLE OF CONTENTS

	Page
ABSTRACT	ii
LIST OF TABLES	v
LIST OF FIGURES	vi
ACKNOWLEDGEMENTS	viii
Chapter	
I. INTRODUCTION	1
I.1 General Introduction	1
I.2 Geographical Description	1
I.3 Oceanographic Data	3
II. CHARACTERISTICS OF THE RUPERT-HOLBERG BASIN WATERS .	6
II.1 Monthly Variability in the Physical Properties	6
II.2 River Runoff and Precipitation	11
II.3 Tidal and Fresh Water Inflow Volumes	11
II.4 Discussion of Data	16
III. ENERGY CONSIDERATIONS	24
III.1 Energy Input	24
III.2 Energy Required for Mixing	27
III.3 Comparison of Energy Input to Energy Required for Mixing	29
IV. DESCRIPTIVE MODEL	30
IV.1 A Model	30
IV.2 Discussion	30

	Page
V. THERMAL MICROSTRUCTURE MEASUREMENTS	34
V.1 Introduction	34
V.2 General Discussion of Thermal Microstructure .	38
V.3 Microstructure in the Rupert-Holberg Basin . .	45
VI. COMPARISON WITH OTHER SHALLOW SILLED INLETS	52
VII. CONCLUSION	55
REFERENCES	57

LIST OF TABLES

TABLE	Page
I. Comparison of the volumes of the Rupert-Holberg basin to the estimated tidal prism and fresh water inflow	15
II. Energy required for mixing of water from Quatsino Narrows into the Rupert-Holberg basin during the times of the mine conducted surveys	28

LIST OF FIGURES

FIGURE		Page
1.	Map of Rupert and Holberg Inlets	2
2.	Quatsino Narrows	4
3.	Monthly values of temperature, salinity and dissolved oxygen content at Station B, in Holberg Inlet.	7
4.	Monthly values of temperature, salinity and dissolved oxygen content at Station D, in Quatsino Sound	9
5.	Depth profiles of temperature, salinity and dissolved oxygen content for Station B, in Holberg Inlet and Station D, in Quatsino Sound during September 1971 and February 1972.	10
6.	Daily precipitation recorded at the mine site and the daily discharge from the Marble River.	12
7.	Weekly and monthly means of precipitation recorded and the mine site.	13
8.	Weekly and monthly means of the Marble River outflow.	13
9.	Comparison of air temperatures with sea surface temperatures	17
10.	Chlorophyll "a" measurements at Station A in Rupert Inlet.	20
11.	Plots of constant σ_t surfaces for UBC and POG data	23
12.	Schematic diagram showing flow conditions between Quatsino Sound and the Rupert-Holberg basin during flood and ebb tide conditions	25
13.	Diagram explaining several of the constituents found in equation (1)	31
14.	Map showing location of microstructure measurements within Rupert and Holberg Inlets	35
15.	Tidal record at Coal Harbour on Holberg Inlet showing the time at which the microstructure measurements were taken.	36

FIGURE	Page
16. A region of stirring observed during drop number 14	39
17. Temperature gradient associated with thermal interface on drop number 21.	40
18. "Older" interfaces observed in Rupert Inlet during drop number 16	41
19. A turbulent intrusion during drop number 23	43
20. Microstructure associated with the mixed layer and the thermocline in Holberg Inlet	44
21. Comparison of the central and outboard thermistors from traces taken during drop number 22	46
22. Deep stirring found opposite Quatsino Narrows on drop number 22	48
23. Deep stirring in Rupert Inlet during drop number 18	48
24. Map of Fortune Channel	54

ACKNOWLEDGEMENTS

I am sincerely grateful to all who have assisted in the preparation of this thesis. I would especially like to thank my supervisor, Dr. T. R. Osborn for the guidance and encouragement he has given me. Also my thanks to Dr. G. L. Pickard for his many helpful comments and his criticism of this manuscript. Professor J. B. Evans was most helpful in making available the data collected by Utah Mines. The help of Mr. C. Pelletier of Utah Mines has been much appreciated. I am also grateful for the co-operation from all the members of the Institute of Oceanography of UBC.

Finally, I wish to thank the National Research Council of Canada who have supported me personally during the last two years of this study.

CHAPTER I

INTRODUCTION

I.1 General Introduction

Industrial, scientific and public interest in Rupert and Holberg Inlets was generated during 1970 with the application and subsequent granting of a permit to discharge wastes from a copper-molybdenum mine into the bottom of these inlets. To determine the environmental effects of this decision, those processes which control the natural phenomena within this region must be understood.

Although several published data reports exist for the Rupert-Holberg system, discussion of its physical oceanography has been limited to brief comments in a general description of Vancouver Island inlets by Pickard, (1963). The influence of fresh water inflow, the uniformity of the water properties and the high oxygen values in the deep water were mentioned. It is in these respects that Rupert and Holberg differ most significantly from other inlets in British Columbia.

This paper attempts to explain the unusual uniformity of the water properties and their monthly changes.

I.2 Geographical Description

Rupert and Holberg Inlets are located near the northern end of Vancouver Island (Fig. 1) and possess a shape typical of British Columbia fjords (Pickard, 1956) being elongated, narrow bodies of water having roughly parallel sides. Rupert Inlet is 10 kilometers long, 1.8 kilometers wide and has a mean mid-channel depth of 110 meters. Holberg Inlet is 34 kilometers long, 1.3 kilometers wide and has a mean mid-

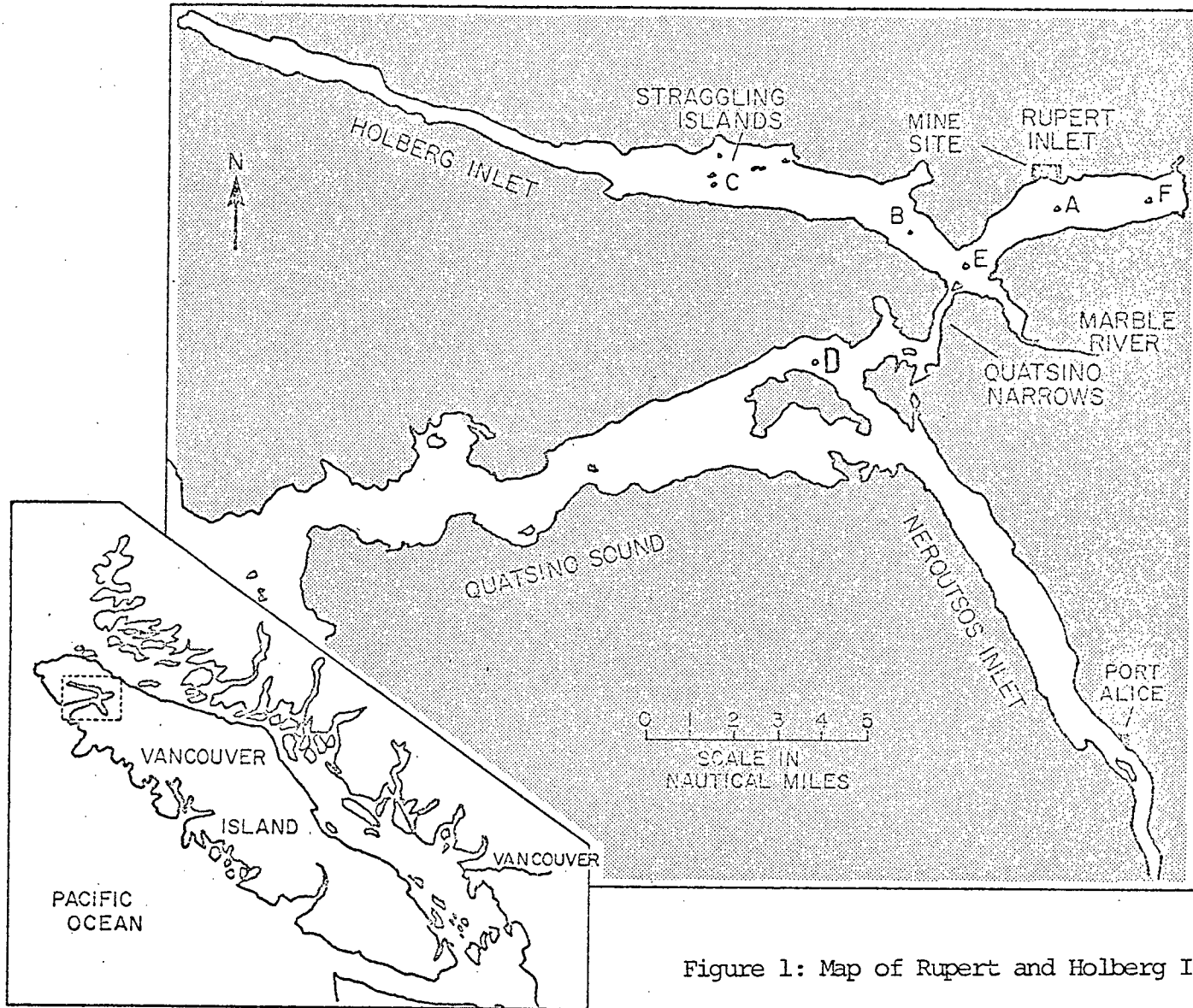


Figure 1: Map of Rupert and Holberg Inlets

channel depth of 80 meters (Pickard, 1963). Together they form a basin of 170 meters maximum depth which is separated from Quatsino Sound and Neroutsos Inlet by Quatsino Narrows. This restriction is a long, narrow channel with a sharp bend at its southern extreme. Its depth decreases northward, culminating in the sill or minimum depth of 18 meters west of Makwazniht Island (Fig. 2).

The principal river affecting the water properties of the Rupert-Holberg basin is the Marble River. It has a drainage area of 512 kilometers², flowing from Alice Lake and entering Rupert Inlet near the junction with Holberg and Quatsino Narrows. This discharge location presents a different situation to that of the typical inlet in which the fresh water enters near the head.

I.3 Oceanographic Data

The oceanographic data used in this study have been collected by three agencies.

The Institute of Oceanography at the University of British Columbia has conducted three cruises into the Rupert-Holberg area. A survey including Quatsino Sound-Neroutsos Inlet was undertaken in May of 1959. Two cruises investigating only Rupert and Holberg were conducted during 1971, one in March, at which time thermal microstructure measurements were taken, and the other in April.

During the years 1965-67, the Pacific Oceanographic Group of the Fisheries Research Board of Canada, Nanaimo, British Columbia (Waldichuk et al., 1968) conducted an extensive survey of several inlets along the west coast of Vancouver Island which included the Quatsino Sound Region. Surveys during August 1957, November 1962 and August 1966, included

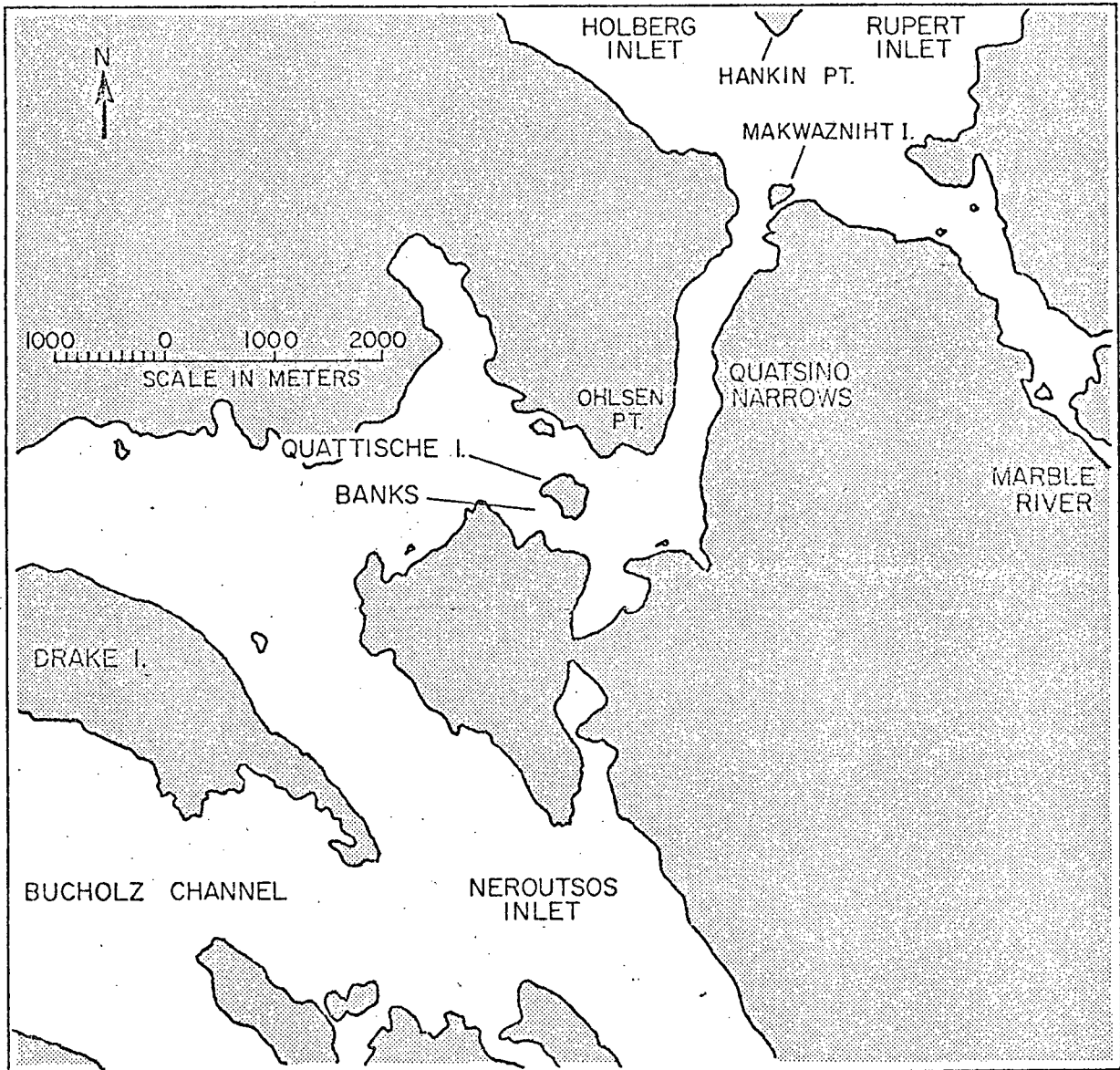


Figure 2: Quatsino Narrows

stations in Rupert and Holberg Inlets.

A programme to determine the effects of the copper-molybdenum mine was begun in the spring of 1971 and is presently scheduled to run until September 1976. Monthly surveys, encompassing six stations (Fig. 1), included observations of temperature, salinity and dissolved oxygen. After June 1972, salinity and dissolved oxygen were measured once every three months. Temperature was recorded using an Applied Research Austin Model ET 100 Marine Thermometer until March 1972, after which reversing thermometers were used. Salinity and dissolved oxygen were determined by titration using the methods described by Strickland and Parsons (1968). All data from the mine monitoring surveys were made available through Professor J. B. Evans, Chairman of the Mineral Engineering Department of The University of British Columbia.

CHAPTER II

CHARACTERISTICS OF THE RUPERT-HOLBERG BASIN WATERS

II.1 Monthly Variability in the Physical Properties

Plots of the monthly values of temperature, salinity and dissolved oxygen content for several depths at Station B are shown in Fig. 3. The data collected during the surveys conducted by the mine show uniform distribution of these properties within Rupert and Holberg Inlets and hence this station is representative of the entire basin.

The temperature throughout the water column changes steadily with a minimum in early spring and a maximum in late summer or early autumn. Within Holberg the maximum temperature in the deep water occurs during early October whereas in Rupert and at Station E the maximum is found at the beginning of September. Below 30 meters, the water in Rupert Inlet during September is approximately 0.2°C higher than at an equivalent depth at Station B. During October it is 0.2°C lower.

Salinity shows more variability with a general trend of high in mid-summer and late winter and low in early spring and late autumn. Surface salinities at Station B (not plotted) vary between 12‰ and 31‰, while below 30 meters salinities vary from 29‰ to 32‰. Below 30 meters, the difference between maximum and minimum salinity is 3‰, independent of depth.

Monthly changes of the order of 1‰ are not uncommon. As density (and σ_t) is primarily dependent upon salinity, the decreases in salinity correspond to decreases in its density.

The dissolved oxygen content tends towards high values in winter and spring, with lower values during summer and autumn. Significant short

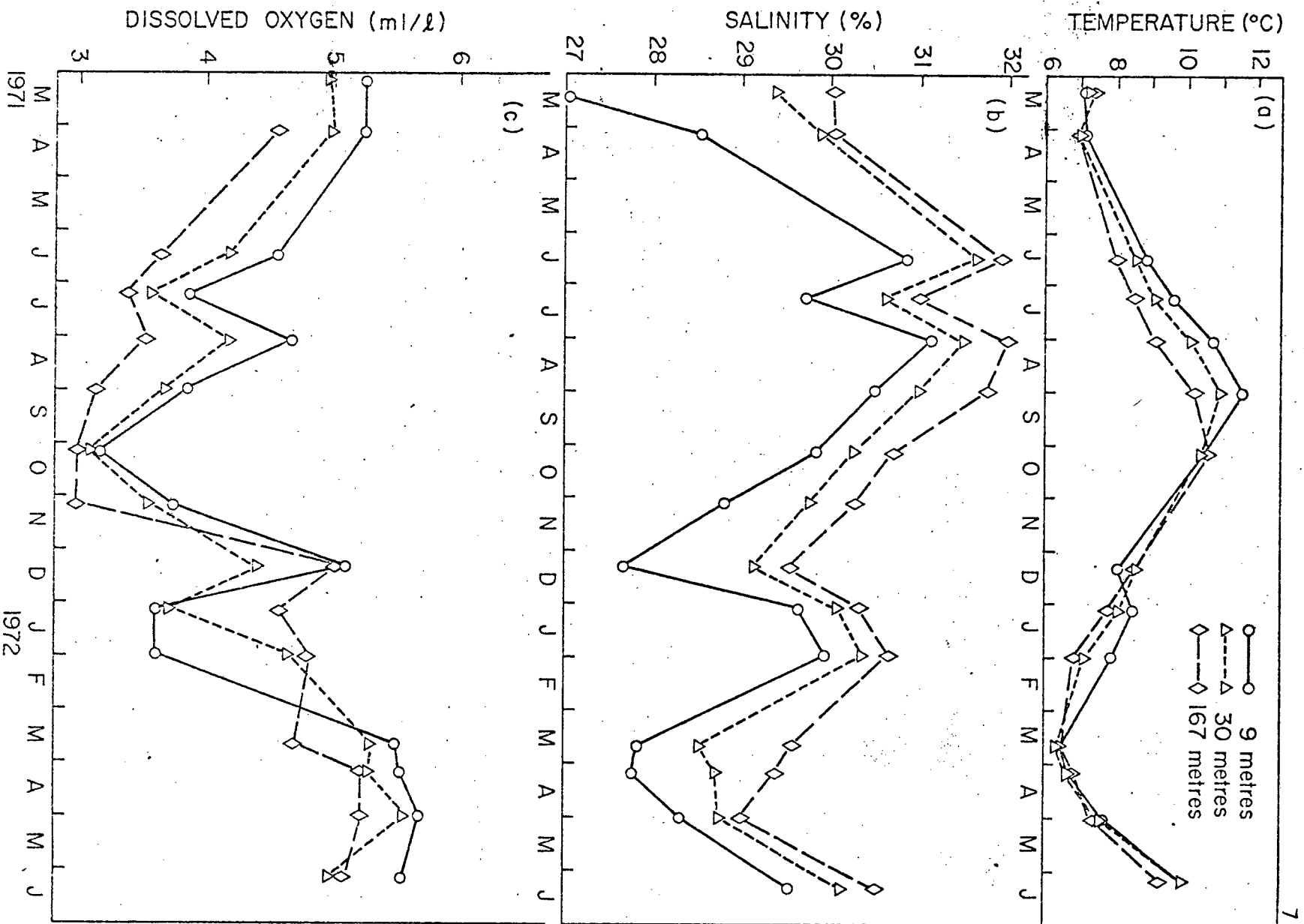


Figure 3: Monthly values of temperature (a), Salinity (b) and dissolved oxygen content (c) at Station B in Holberg Inlet.

term increases in oxygen appear during August 1971 and December 1971.

Monthly data for Quatsino Sound, Station D, are displayed in Fig. 4. The variability of the upper layers, surface to 60 meters, is similar to that within Rupert and Holberg. The bottom water (60 to 116 meters) has different characteristics with a maximum in January and a smaller temperature range than the upper layers.

Except during the autumn months, the salinity trends at station D, for all depths are alike and follow a pattern close to that of the basin. The difference in the salinities between the top and bottom layers is greater at station D, than in the deeper Rupert-Holberg basin. The magnitude of the salinity fluctuations decrease with depth at station D.

Although a wider range of oxygen values exist within the water column at station D, the trends of the oxygen are similar to those found in the basin. A notable increase, especially in the upper layers, occurs during August 1971. Oxygen values at the 30 and 46 meter depths are frequently higher than those found at the 9 meter depth. Cause of this unusual occurrence may result from an influx of low oxygen values in the surface waters of Neroutsos Inlet due to the existence of a pulp and paper mill at Port Alice. The mill is still in operation.

Figure 5 shows the temperature, salinity and dissolved oxygen content profiles at Stations B and D during surveys taken in September 1971 and February 1972. These months are representative of summer and winter structure respectively. All stations within the Rupert-Holberg basin exhibit similar shaped profiles to those of Station B, excepting Station E, where a slightly greater degree to vertical uniformity normally exists.

These profiles indicate that below 30 meters a more homogeneous water body is found in the basin, than in Quatsino Sound.

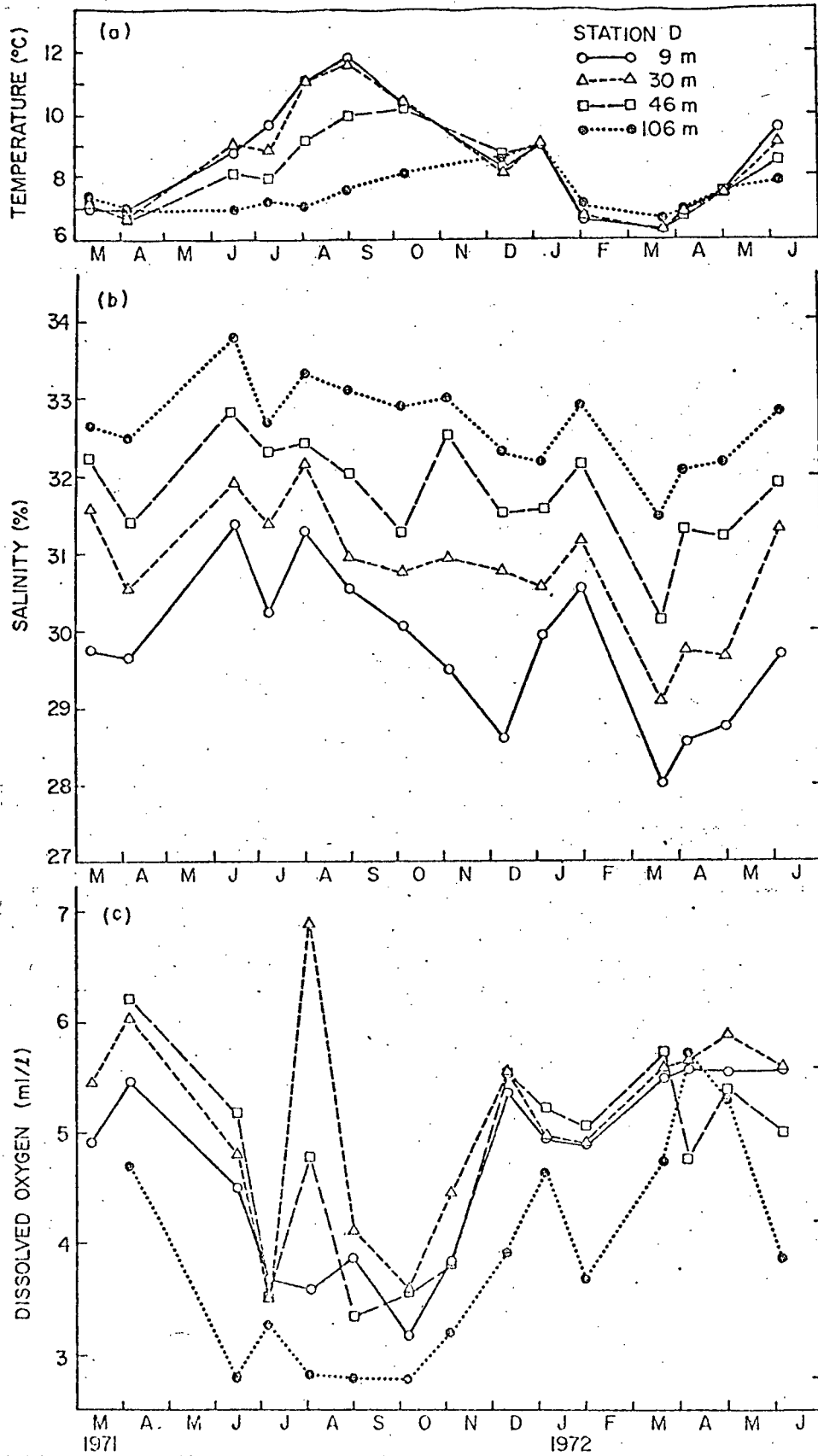


Figure 4: Monthly values of temperature (a) salinity (b) and dissolved oxygen content (c) Station D in Quatsino Sound

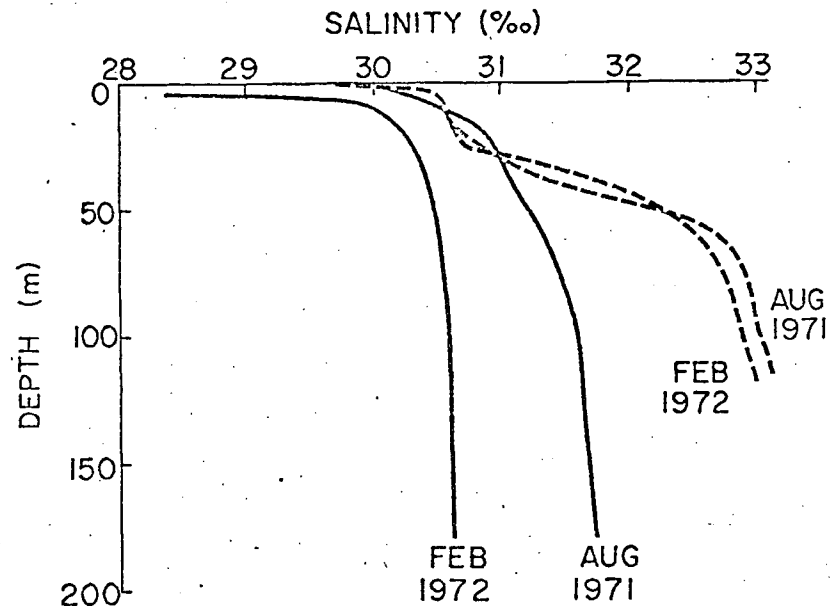
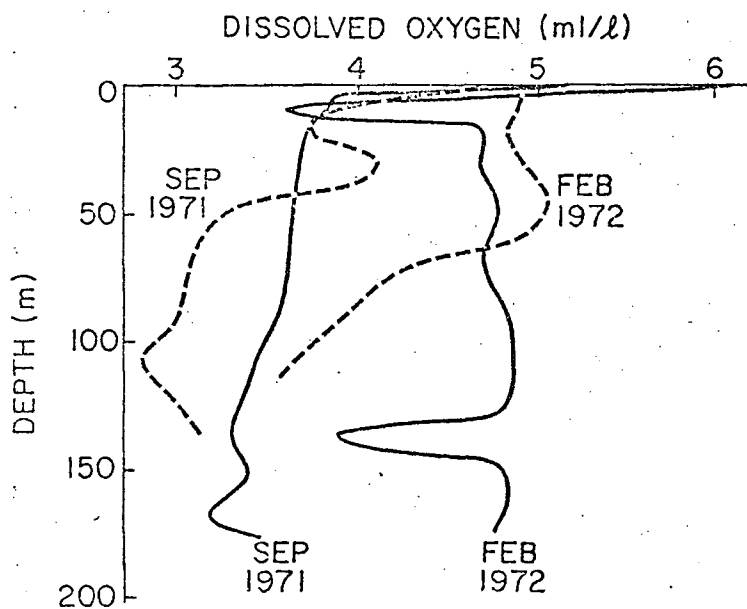
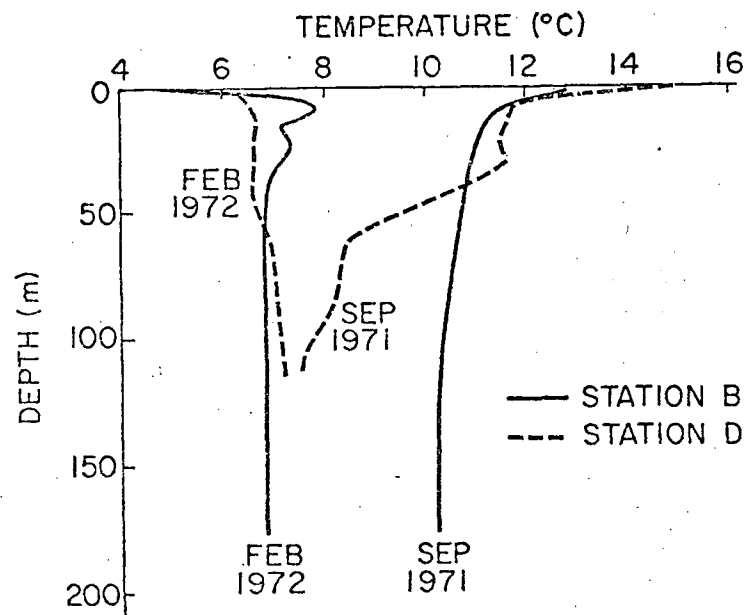


Figure 5: Depth profiles of temperature (a), salinity (b), and dissolved oxygen content (c) for Station B in Holberg Inlets and Station D in Quatsino Sound during September 1971 and February.

Studies by Pickard (1961 , 1963) indicate the water properties in most British Columbian inlets are not as uniform as those found in the Rupert-Holberg basin.

II.2 River Runoff and Precipitation

The close correspondence between precipitation and the Marble River runoff is shown in Figures 6, 7 and 8. The daily values of precipitation and river discharge during the months of October and November, 1971 are displayed in Fig. 6. The precipitation was recorded at the mine site. The discharge data were supplied by J.S. Areneault of the Canadian Fisheries Service (personal communication). Generally, fluctuations in precipitation produce corresponding fluctuations in the discharge. However, the actual relationship between these two features is non-linear. The discharge data reflect the possibility of a filtering effect on the precipitation, for example, several of the low frequency fluctuations in precipitation are not evident in the discharge data. A lag of approximately one to two days exists between peaks in rainfall and river discharge.

Figures 7 and 8 show the weekly and monthly means of precipitation and Marble River discharge for all the available data between March, 1971 and June, 1972. The sources of data were the same as for Fig. 6. The peak in precipitation during early September is of questionable magnitude. As in the daily data, both the weekly and monthly means show a correspondence between precipitation and river runoff.

II.3 Tidal and Fresh Water Inflow Volumes

A comparison of the basin volume to the tidal prism and fresh water

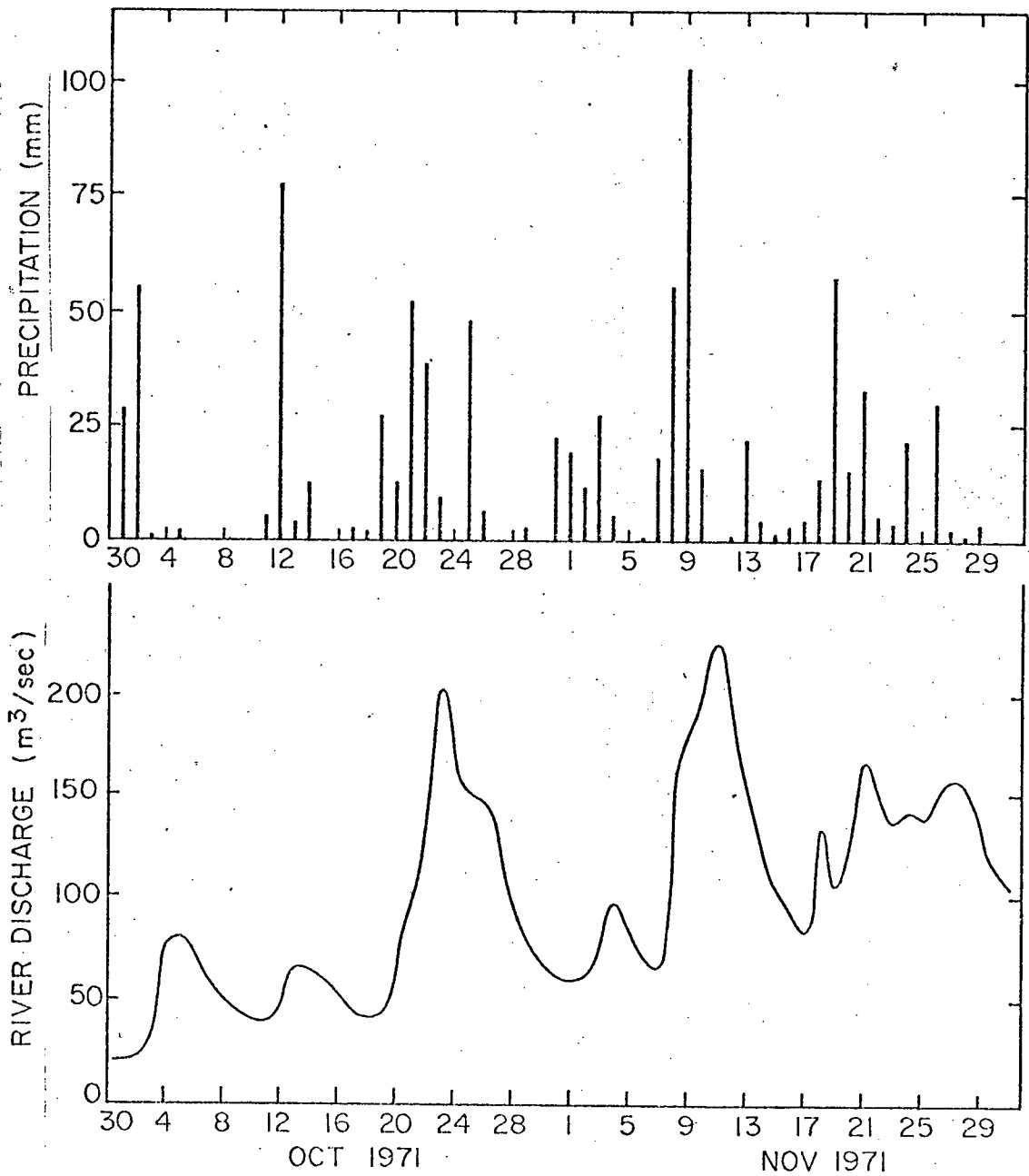


Figure 6: Daily precipitation recorded at the mine site and the daily discharge from the Marble River.

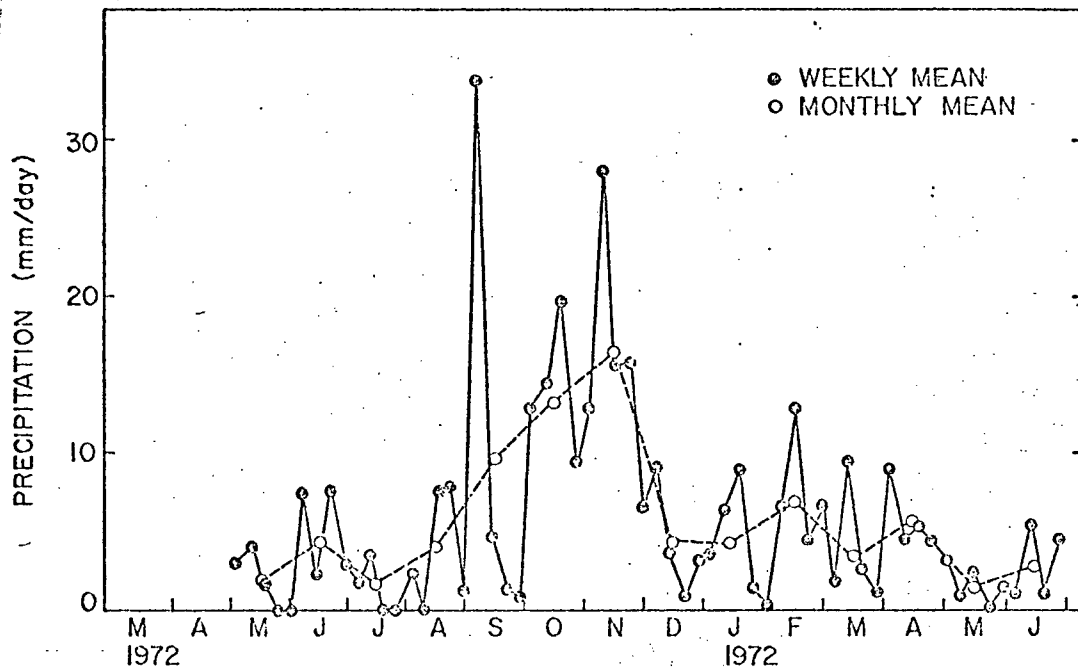


Figure 7: Weekly and monthly means of precipitation recorded at the mine site.

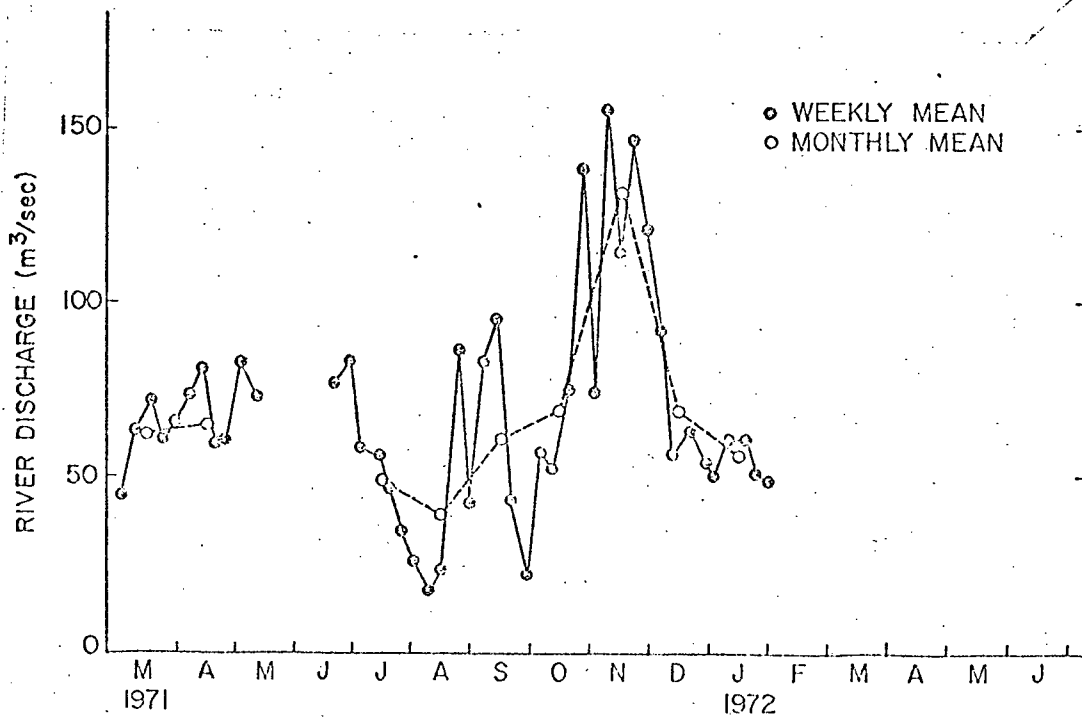


Figure 8: Weekly and monthly means of the Marble River outflow.

inflow is given in Table 1. The volumes of Rupert and Holberg Inlets are calculated on the basis of a rectangular basin. The mean values previously quoted are used for the dimensions. The tidal prism is defined as the surface area of the inlets multiplied by the increase in depth due to the tide. The average tidal prism is determined using a tide of 2.8 metres while an increase of 4.2 metres is used for maximum conditions. These are the ranges for Coal Harbour (Canadian Tide and Current Tables (1971)).

A drainage area of approximately 580 km² surrounds Rupert and Holberg Inlets, excluding the Marble River drainage of 512 km². No major river system exists within the former area. Thus based entirely on the relative sizes of the drainage areas, the total volume of the fresh water flow into the basin is assumed to be approximately twice that of the Marble River. The average discharge is tabulated from the total of all daily measurements divided by the number of days. The maximum inflow occurred November 11, 1971.

Table 1.

(a) Volume of Rupert-Holberg Basin and Quatsino Narrows	
	Volume (10^6 m^3)
Rupert Inlet	2000
Holberg Inlet	3400
Rupert-Holberg Basin	5400
Quatsino Narrows	30
(b) Volume of Tidal Inflow (Tidal Prism)	
	Volume (10^6 m^3 / tidal cycle)
Average Conditions	170
Maximum Conditions	260
(c) Volume of Fresh Water Inflow	
	Volume (10^6 m^3 /day)
Average Conditions	12
Maximum Conditions	40

II.4 Discussion of Data

The vertical uniformity of temperature, salinity and dissolved oxygen content, accompanied by their month to month variability suggests a process operating on a time scale of less than a month which is capable of increasing or decreasing the salinity, temperature and density of the entire basin water. Increasing deep salinities and densities can be attributed to intrusions into the basin of denser water from Quatsino Sound. However the periods of decreasing bottom densities require an influx of energy to raise the potential energy of the water within the basin.

Comparison of the sea surface temperatures at station B with the monthly mean air temperatures and the mean air temperatures 3 days immediately preceding the sea measurements are shown in Fig. 9. All air temperatures were recorded at the mine site. A closer resemblance between the sea surface temperatures and the 3 day average of the air temperatures implies the surface layers are controlled by short term changes of air temperature. Determination of the actual relationship requires further data. It seems safe to assume however that the temperature of the surface layers are primarily controlled by solar influences. The similarity in temperature trends between the deep water and the surface layers (Fig. 3b) suggests these solar influences are felt throughout the water column. This further suggests the existence of a vertical heat transfer mechanism within the basin.

The likeness between the monthly fluctuations of surface salinity and those of the deeper water within the basin (Fig. 3b) infers the existence of a mixing process. These salinity changes are inversely related to fluctuations in river discharge (Fig. 8) and hence also precipitation (Fig. 7). The time response of the basin water to discharge changes appears to be between one and four weeks.

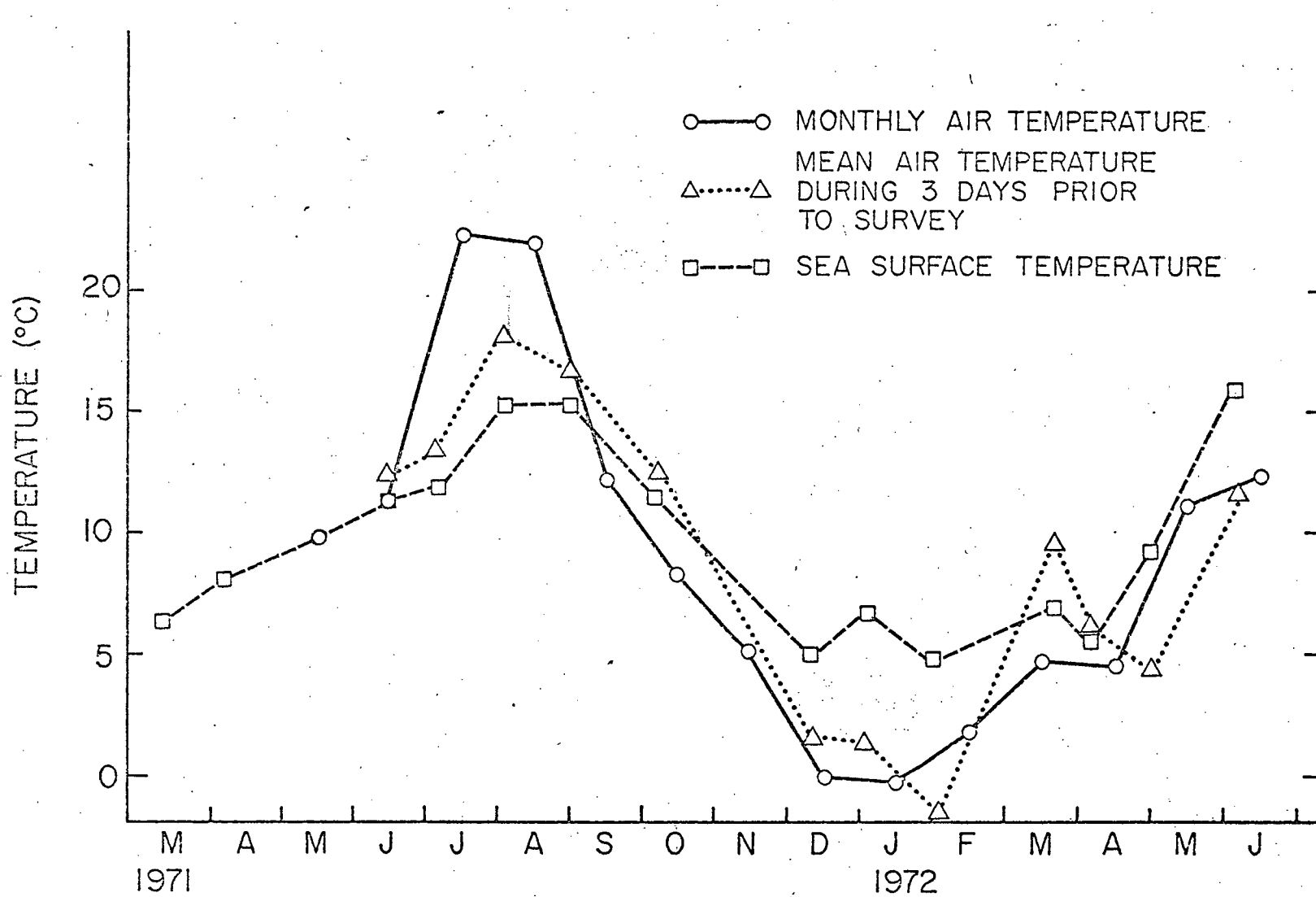


Figure 9: Comparison of air temperatures with sea surface temperatures.

More frequent salinity data are required to establish an accurate time response.

Pickard (1961) has described seasonal variations in Bute Inlet and Indian Arm where salinity fluctuations are observable to 30 and 50 meters respectively while temperature changes are apparent to 100 meters depth in both. The extent of the seasonal variability in the Rupert-Holberg Basin thus indicates a different mixing process than normally found in British Columbian inlets.

Assuming similar conditions of solar radiation and rainfall exist on both sides of Quatsino Narrows, the temperature and salinity distributions of the upper layers of Quatsino Sound and Rupert-Holberg Inlets would have marked resemblance. Thus mixing of surface water from either side of the narrows into the basin would produce the same result. The question as to the relative amounts of water from either source that are mixed into the Rupert-Holberg Basin can only be answered after determining the cause of the mixing process.

The near uniformity of the oxygen content throughout the water column implies frequent mixing within the basin. The lower values during the summer and autumn may be attributed to an influx of low oxygenated water from the Pacific Ocean into Quatsino Sound. Lane (1962) has shown upwelling to occur during summer along the coast of Vancouver Island (off Amphitrite Point) and then move into the shelf. Pickard (1963) reports evidence of upwelling off Quatsino Sound but with no distinct seasonal variations. The rise in salinity during June, 1971 and the low temperatures within the deep water during the summer at Station D are additional evidence for upwelling. Also during the summer, sinking organic matter, caused by an increase in

biological activity, may use up oxygen in the deeper waters. An increase of chlorophyll (Fig. 10) indicates the high August oxygen values to be associated with a plankton bloom.

Investigation into tidal effects leads to a possible explanation of the mixing. Assuming complete and instantaneous mixing with an average tidal volume per tidal cycle, then in one month about 15% of the original water will remain in the basin. The average monthly fresh water discharge is 1/15 of the entire volume of the basin. During a high runoff month this volume inflow doubles. Mixing the average fresh water inflow into the basin throughout the water column would produce salinity changes of approximately 2‰ .

Excellent conditions for mixing exist within Quatsino Narrows due to its geographical configuration (Fig. 2). The majority of water flowing into or out of Quatsino Sound must pass through a narrow channel north of Quattische Island as shallow banks prohibit the movement of large volumes of water south of the island. On a flood tide, this effect produces a narrow eastward flowing current which passes north of Quattische Island. A large deflection is needed to redirect the current northward towards Rupert and Holberg. Its momentum however, resists any immediate redirection of flow and causes the current to continue its approach towards the eastern shore of Quatsino Narrows. Surface current data (Canadian Hydrographic Service, 1972) show the current to split near the shore, part moving south to create a large eddy south-east of Quattische Island and part hugging the east shoreline as it heads north through the narrows. Several smaller eddies, produced by indentations along the eastern shoreline are also observed further up the channel.

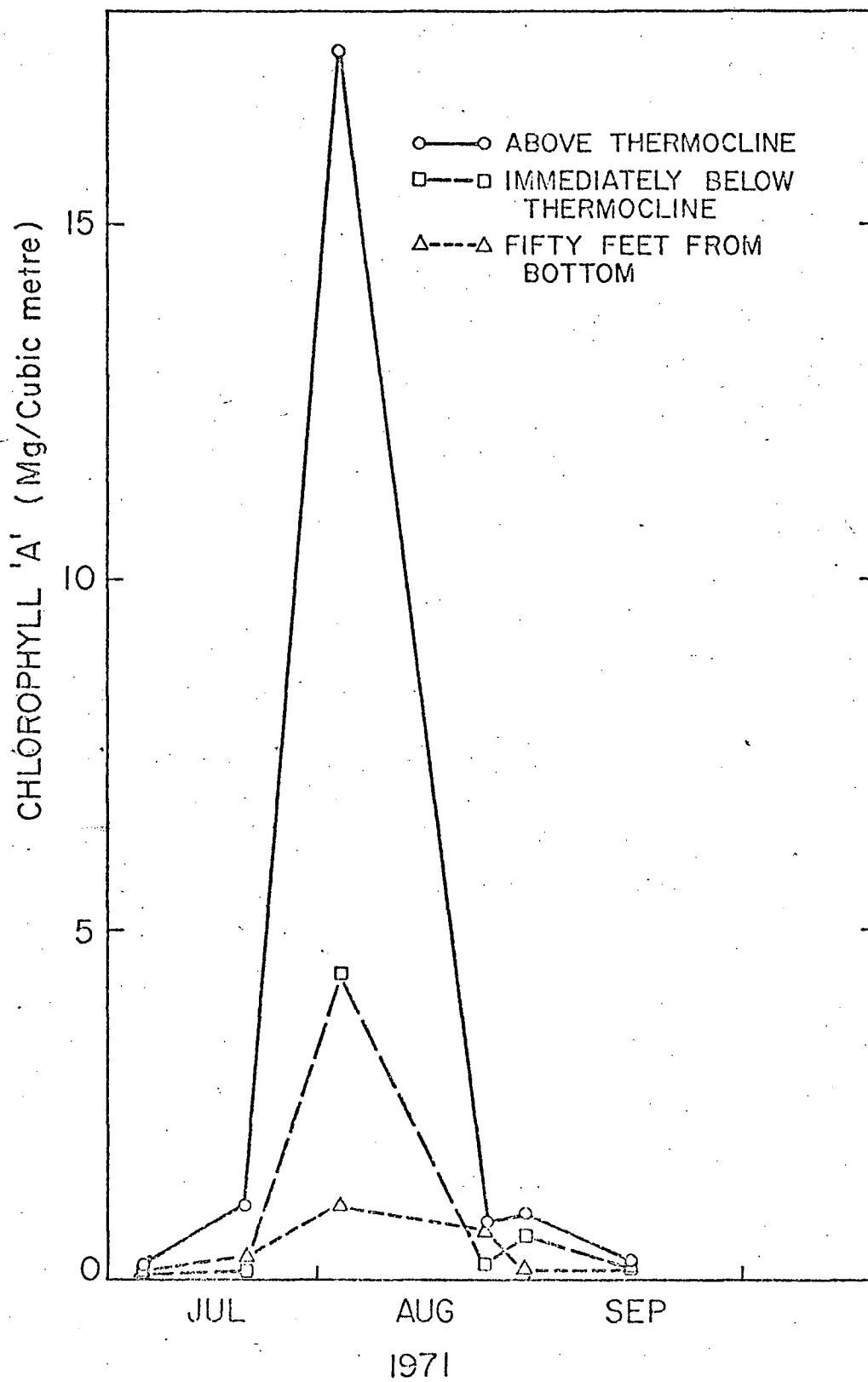


Figure 10: Chlorophyll "a" measurements at Station A in Rupert Inlet.

Data collected in August 1957 (Waldichuk et al., 1968) during high tide suggests that this eddy stirs and mixes the water. Over the 20 meter depth surveyed, the density changed by only 0.27 of a σ_t unit and an instability was present between 9 and 14 meters. The density of the upper 10 meters was greater than that observed at equivalent depths outside the narrows. At 20 meters depth however, the density was slightly less in the narrows than that observed in Quatsino Sound. Mixing will also be associated with eddies. During an ebb tide, similar conditions to that of the flood tide produce mixing within the same region. The upper layers of the Rupert-Holberg basin flow southward through the channel and beyond Ohlsen Point. The required redirection of the flow westward into Quatsino Sound is at first prohibited by the momentum of the flow. The current studies previously mentioned show the formation of a large anticlockwise eddy south-east of Quattische Island and a westward flow past the northern end of this island. Very turbulent water throughout the narrows has been personally observed during both flood and ebb tides.

The volume of Quatsino Narrows, between Makwazniht Island and Quattische Island (Table 1), is approximately one sixth of the average tidal prism. As the tides are semi-diurnal the water within the tidal prism spends approximately 1 hour within the narrows. This allows sufficient time for the mixing, described above, to occur.

Thus the narrows mixes the fresher and denser sections of the upper layer which enters the channel. This mixing results in the density of the water within the narrows being greater than that of the surface layers outside. Upon entering the Rupert-Holberg Basin on a flood tide, this water will sink beneath the less dense, low salinity layer formed by the

Marble River. Less energy is then required to mix this water into the deeper water of the inlet as it is already below or at least partially through the pycnocline.

Plots of isopleths of σ_t are shown in Fig. 11. These enforce the concept of exchange as envisioned above. The bottom waters in the basin are less or at least an equivalent density to the upper 40 meters of water in Quatsino Sound, indicating that changes in the upper layers will likely be reflected by changes in the bottom waters. Although isopleths are drawn smooth through the narrows, the water is probably more homogeneous than indicated for reasons previously discussed.

Observations suggest that the mixing energy is supplied by the tide and the process enhanced by the penetration of the water below the pycnocline.

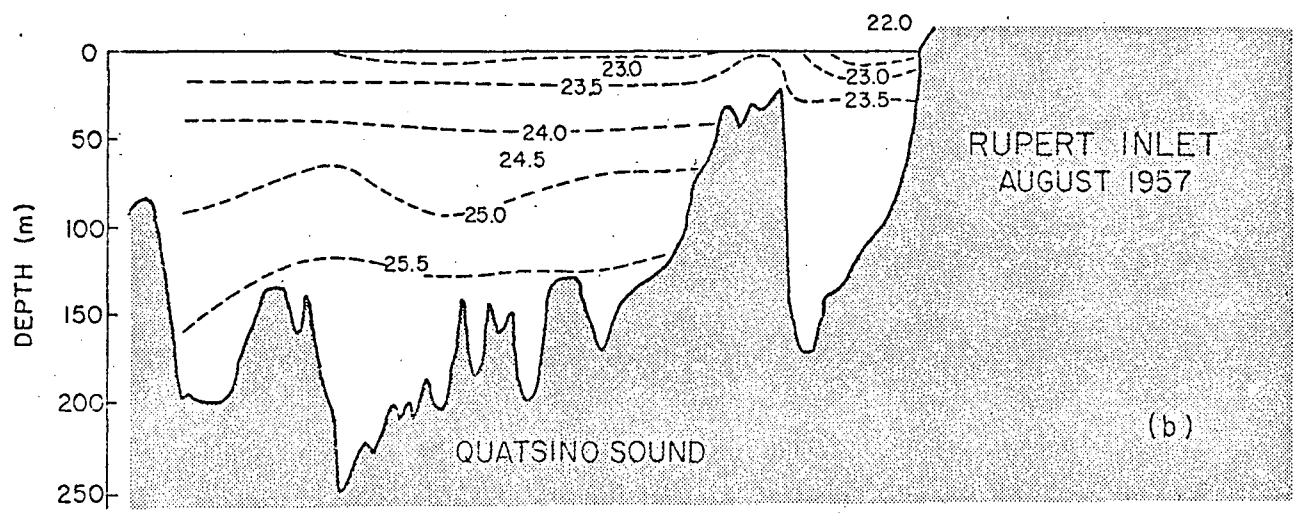
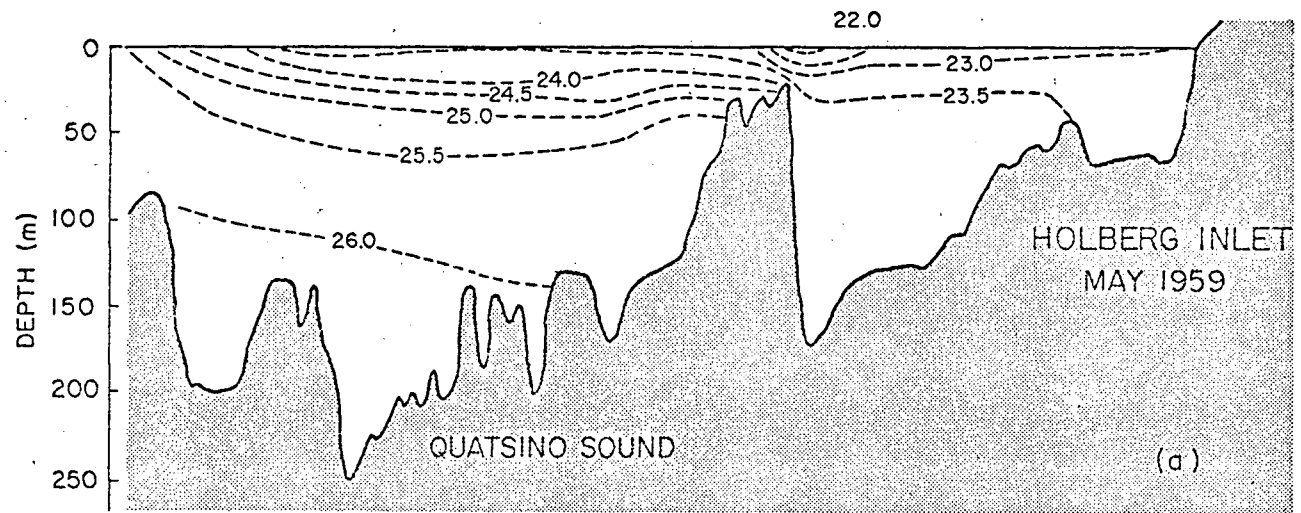


Figure 11: Plots of constant surfaces for (a) UBC data, (Pickard) data and (b) POG data (Waldichuk, et al)

CHAPTER III
ENERGY CONSIDERATIONS

III.1 Energy Input

The rate at which available energy flows into the Rupert-Holberg basin is calculated using the method of Taylor (1919). Consider a given volume of water which at time t is enclosed by a surface area A (extending the entire depth under consideration). The rate at which energy (W) is transported across surface A is

given by:

$$\frac{dW}{dt} = \int \left\{ \rho g \frac{(D+h)}{2} (v \cos \theta) (D+h) \right\} dS + \int \rho (D+h) \frac{(h-D)}{2} (v \cos \theta) dS + \int \frac{\rho v^2}{2} (D+h) (v \cos \theta) dS \quad (1)$$

where h is the tidal height above mean sea level

ρ is the density of the fluid (assumed homogeneous)

g is the acceleration due to gravity

t is the time measured after an arbitrary turn to flood

D is the depth of the sea floor below mean sea level

v is the velocity

θ is the angle between the current direction and the element dS

and dS is the element of length along A (Fig.12).

The first term represents the rate at which work is done by the mean hydrostatic pressure on that portion of fluid originally within A ; the second term is the rate of gravitational potential energy transport across A , with zero potential at mean sea level; and the last term is the rate at which kinetic energy crosses A .

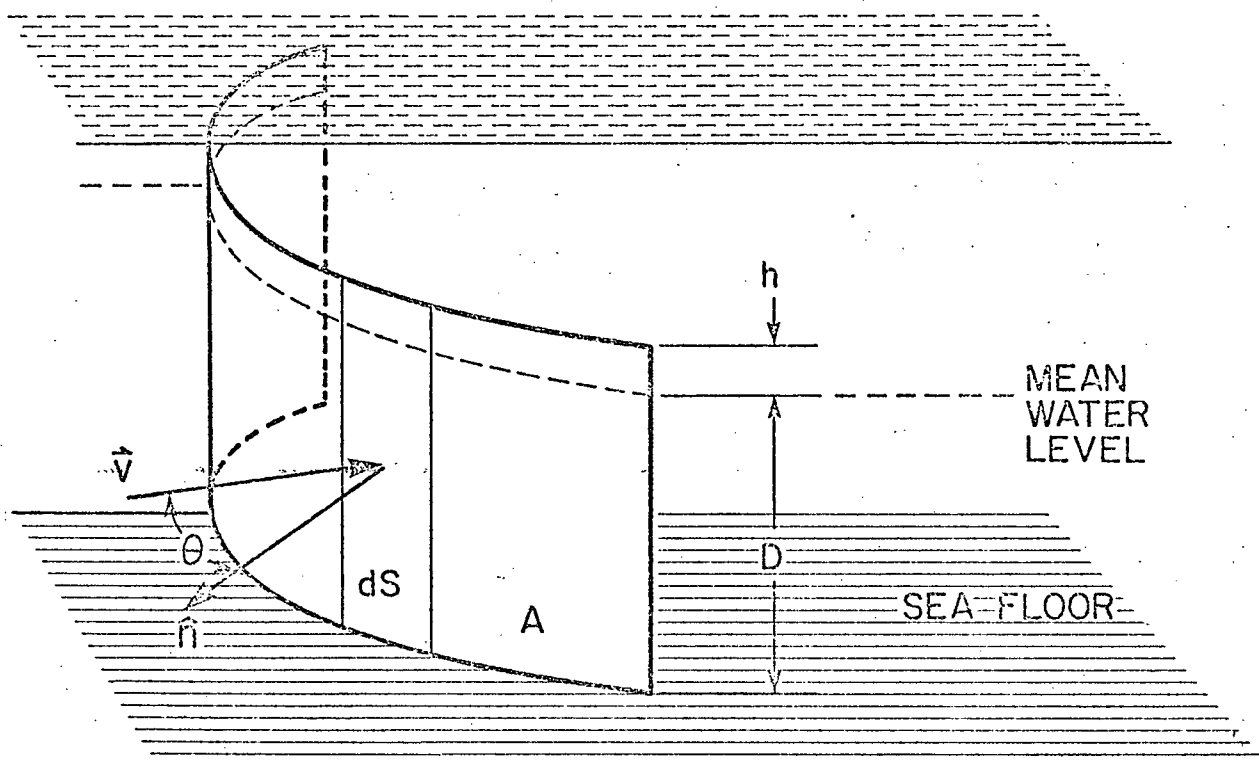


Figure 12 : Diagram explaining several of the constituents found in equation (1).

Combining terms

$$\frac{dW}{dt} = \rho g \int Dh v(\cos\theta) dS + \frac{\rho}{2} \int v(\cos\theta) (2gh^2 + Dv^2 + hv^2) dS \quad (2)$$

Averaging over one tidal cycle this equals the energy dissipated by friction and by raising the gravitational potential energy by mixing. This assumes no net increase of kinetic energy within the basin.

For the Rupert-Holberg system the tidal height and velocity to the first approximation take the form

$$h = H \cos \frac{2\pi t}{T} \quad v = -V \sin \frac{2\pi(t-T_0)}{T}$$

where H is the maximum current velocity,

V is half of the tidal range,

T is the tidal period,

and T_0 is the time difference between high water in Rupert Inlet and turn to ebb at Quatsino Narrows.

Averaging over one tidal cycle, the last three terms disappear and the average rate of energy crossing the sill (U), assuming conditions are uniform across the channel, is given by

$$U = \frac{1}{2} \rho g H V \left(\sin \frac{2\pi T_0}{T} \right) (\cos\theta) DL \quad (3)$$

where L is the length across the sill.

The numerical values of the constituents are

$$\rho = 1.023 \text{ gm/cm}^3 \quad g = 9.8 \text{ m/sec}^2 \quad H = 1.4 \text{ m}$$

$$V = 7.0 \text{ knots} = 3.6 \text{ m/sec} \quad T = 12 \text{ hr. } 25 \text{ min} = 745 \text{ min}$$

$$T_0 = 11 \text{ min} \quad \sin \frac{2\pi T_0}{T} = \sin 5^\circ 18' \approx .09 \quad \theta = 0^\circ$$

$$\cos\theta = 1 \quad D = 20 \text{ m} \quad L = 250 \text{ m}$$

-Substituting into equation (3), the average energy which must be dissipated within the basin by friction and mixing is found to be on the order of 10^7 joules/second. This value multiplied by the tidal period (T) gives 5×10^{11} joules as the total energy to be dissipated during one tidal cycle. The average energy per unit volume of the incoming tidal water is then the total energy divided by the tidal prism and has a value of 3×10^3 joules/meter.³

III.2 Energy Required for Mixing

Energy to overcome the buoyancy force is needed when mixing waters of unequal density. To mix a layer of thickness h_1 and density ρ_1 into a thicker layer h_2 , of density ρ_2 , some mechanism must do an amount of work per unit area of

$$-(\rho_2 g h_2) \cdot \frac{h_1}{2} + (\rho_1 g \frac{h_1}{2}) \cdot h_1$$

which reduces to

$$(\rho_2 - \rho_1) g \frac{h_1 h_2}{2} .$$

To simulate flood conditions in Rupert and Holberg Inlets, a 10 meter layer, whose density corresponds to the 9 meter depth at station D, over a 150 meter layer whose density equals that found at the bottom of the basin is chosen. Table 2 shows the mixing energy per unit volume required assuming it is contained within the upper layer. These values were obtained by dividing the work done per unit area by the thickness of the upper layer.

Table 2

Energy Required for Mixing During Times of Mine
Conducted Surveys

<u>Month</u>	<u>ρ_1 (gm/cm³)</u>	<u>ρ_2 (gm/cm³)</u>	<u>ENERGY</u> <u>(joules/m³)</u>
March 8-10, 1971	1.02333	1.02344	80
April 5-6	1.02326	1.02353	198
June 14-18	1.02434	1.02488	397
July 6-8	1.02332	1.02407	552
Aug 2-4	1.02387	1.02487	736
Sept 1-2	1.02319	1.02440	891
Oct 4-5	1.02306	1.02360	397
Dec 7-11	1.02223	1.02297	528
Jan 3-6, 1972	1.02319	1.02368	360
Feb 1-3	1.02389	1.02405	51
March 17-22	1.02200	1.02325	920
April 5-7	1.02238	1.02306	501
May 1-3	1.02245	1.02257	88
June 5-7	1.02291	1.02359	501

III.3 Comparison of Energy Input To Energy Required For Mixing

On an average, each cubic meter of water within the tidal prism contains excess energy of the order of 3000 joules. If mixing similar to that assumed in the model did occur, then between 50 and 1000 joules per cubic meter of incoming water would be needed. Much energy would be dissipated by molecular viscosity. However if only a small fraction of the available energy per tidal cycle is used in raising the potential energy, its continual injection into the basin would still produce the required mixing.

Energy between 250 and 3000 joules per cubic meter of incoming water would be needed to mix the surface water from Quatsino Sound into the basin. Thus the mixing within the narrows decreases the required energy for mixing in the basin by approximately 2 to 3 times.

CHAPTER IV
DESCRIPTIVE MODEL

IV.1 A Model

A descriptive model is developed to visualize clearly the processes which occur. Figure 13 shows a diagrammatic picture of flood and ebb tide conditions. A three layer system is considered in Quatsino Sound: A, an upper layer; B, the pycnocline region; and C, the bottom water. Layer D, represents the homogeneous water within Quatsino Narrows. Rupert and Holberg consist of a low salinity layer, E, above a layer extending to the basin floor, F. The order of increasing density is E,A,D,F,B and C. Slight modifications to this order are discussed later.

During a flood tide, layers A and B are forced into Quatsino Narrows where they mix to homogeneity, thus producing more of layer D. At the opposite end of the narrows, layer D enters into the Rupert-Holberg Basin, sinking below the low salinity layer, E, and mixing into the region F. The degree of mixing depends upon the density difference between D and F and the available energy.

On an ebb tide, layer E and part of layer F move into the narrows to become well mixed. This water eventually passes into Quatsino Sound at a depth dependent upon the density difference between it and layers A and B.

IV.2 Discussion

This model illustrates how water from the narrows is injected into the basin. The momentum of the incoming tide pushes aside the low salinity layers of the basin between the narrows and Hankin

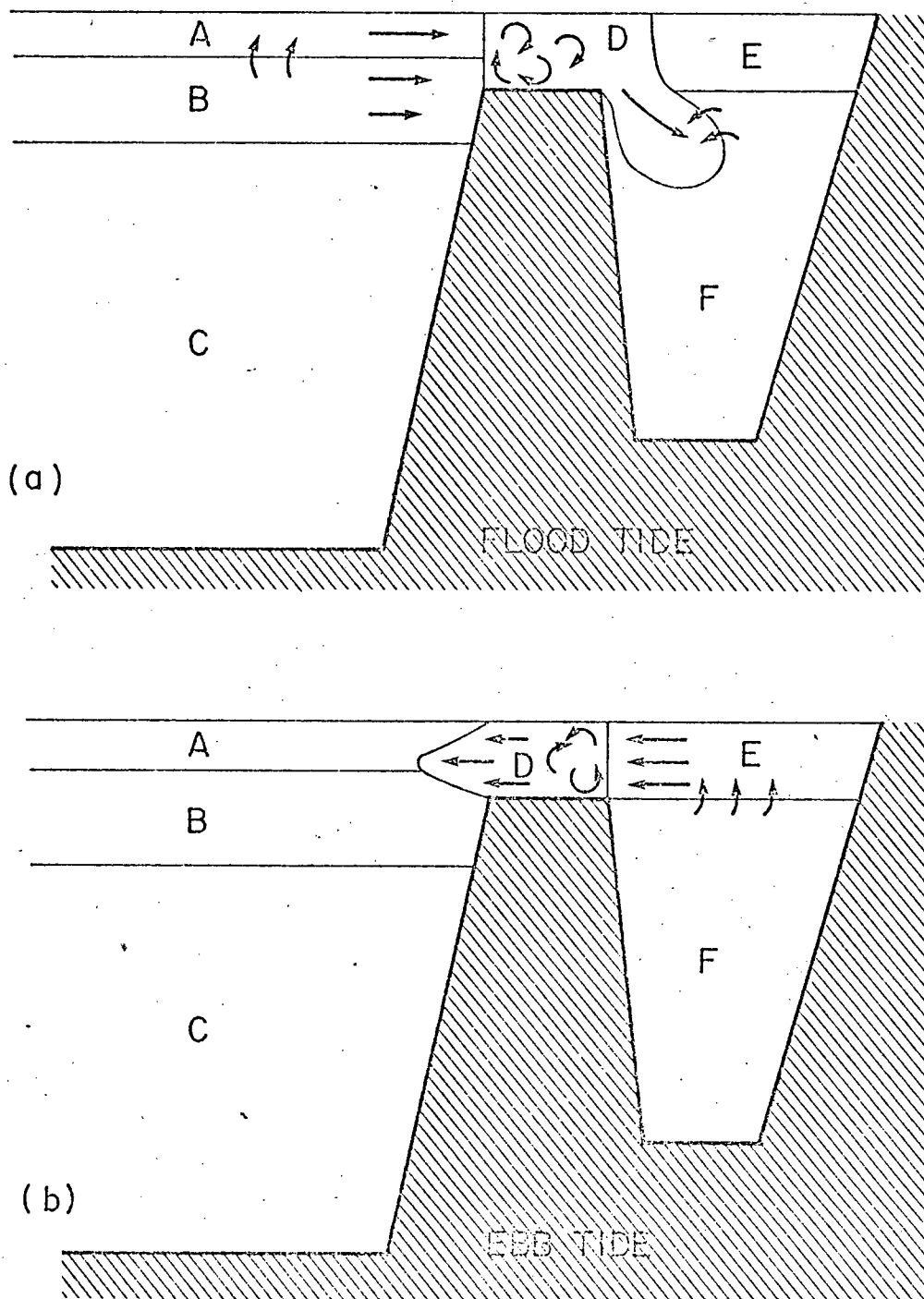


Figure 13: Schematic Diagram showing flow conditions between Quatsino Sound and the Rupert-Holberg basin during (a) flood tides and (b) ebb tides.

Point. Visual observations show turbulent water within this area during a flood tide and contrasts with the apparent calm conditions surrounding it. The density difference eventually causes the incoming water to sink below the fresher layer. Thermal microstructure measurements (Chapter V) suggest that the majority of the tidal inflow is then stirred into the basin just beyond the sill. This causes the greater vertical uniformity observed at Station E. Internal mixing could then proceed by pressure gradient currents due to the density difference between this region and the rest of the inlet.

During ebb conditions the fresh water layer, the majority of which originates from the Marble River, flows out toward the narrows entraining the deeper more saline water into it. A flow is required to replace the saline water. During flood tides, the injection of the water beneath the low salinity layer just beyond the narrows necessitates a subsurface flow to spread the water throughout the basin. It is noted that normal estuarine circulation requires a subsurface up-inlet flow to replace the saline water entrained into the continual outflowing surface layer (Tully, 1949). However, lack of such a regular outflow, due to the major fresh water inflow being concentrated near the mouth, changes the nature of the circulation from that of the typical inlet.

The depth and water properties of the layers described in the model undergo continual change. River runoff, solar radiation, winds, precipitation and, in the case of Quatsino Sound, outside influences from the Pacific Ocean all combine to modify these layers. The model presents an influx of less dense water into the basin. It also allows for deep flushing and mixing. If layer A is very shallow or is denser than the

basin water, the tidal inflow would plunge over the sill, dropping to the basin floor. The observed increases in the density of the deep water in the basin are most likely to have occurred through gradual rather than large scale changes of this nature. A continual increase in the density of the water flowing through Quatsino Narrows, caused by decreasing runoff, would result in a corresponding increase in the density of the deep water in the basin. Sudden large scale decreases in the density of the deep water would seldom be expected. However, upwelling off the coast and subsequent inflow into Quatsino Sound might produce the necessary conditions for this to happen.

The ebbing waters from Quatsino Narrows are assumed to flow into Quatsino Sound at a depth dependent upon the density difference between the incoming and existing waters. If this depth is shallow, the water could re-enter the narrows on the following flood tide. Existing circulation patterns may remove it entirely. Further data are required to determine the actual process which occurs.

CHAPTER V

THERMAL MICROSTRUCTURE MEASUREMENTS

V.1 Introduction

Thermal microstructure refers to temperature and temperature gradient fluctuations on the scale of a few centimeters. Measurements of this nature were taken in Rupert and Holberg Inlets between March 6 - 10, 1971. Twenty successful recordings were obtained at nine separate locations throughout the basin (Fig. 14). Figure 15 shows the state of the tide at the time the measurements were taken. Four other recordings were unuseable due to technical problems or instrument calibration. The instrument used contained two thermistors separated horizontally by one-half meter and attached to the bottom of a free-falling, rotating instrument package (Osborn, 1973). The fall speed was on the order of 20 centimeters per second. One thermistor mounted along the central axis of the instrument recorded the vertical temperature profile. The other thermistor recorded the temperature in a helical path about the central axis. Absolute temperatures are found by comparison of the instrument's temperature signal to the temperatures recorded previously by reversing thermometers. Thus small errors may exist in these absolute values, however the temperature differences are accurate. The temperature signals were differentiated and sent through a 25 hertz low pass filter to obtain the temperature gradients. The noise level of the gradients is 4.25×10^{-3} C°/cm.

Since a general account of microstructure in inlets has not yet been published the feature of thermal microstructure in inlets are discussed.

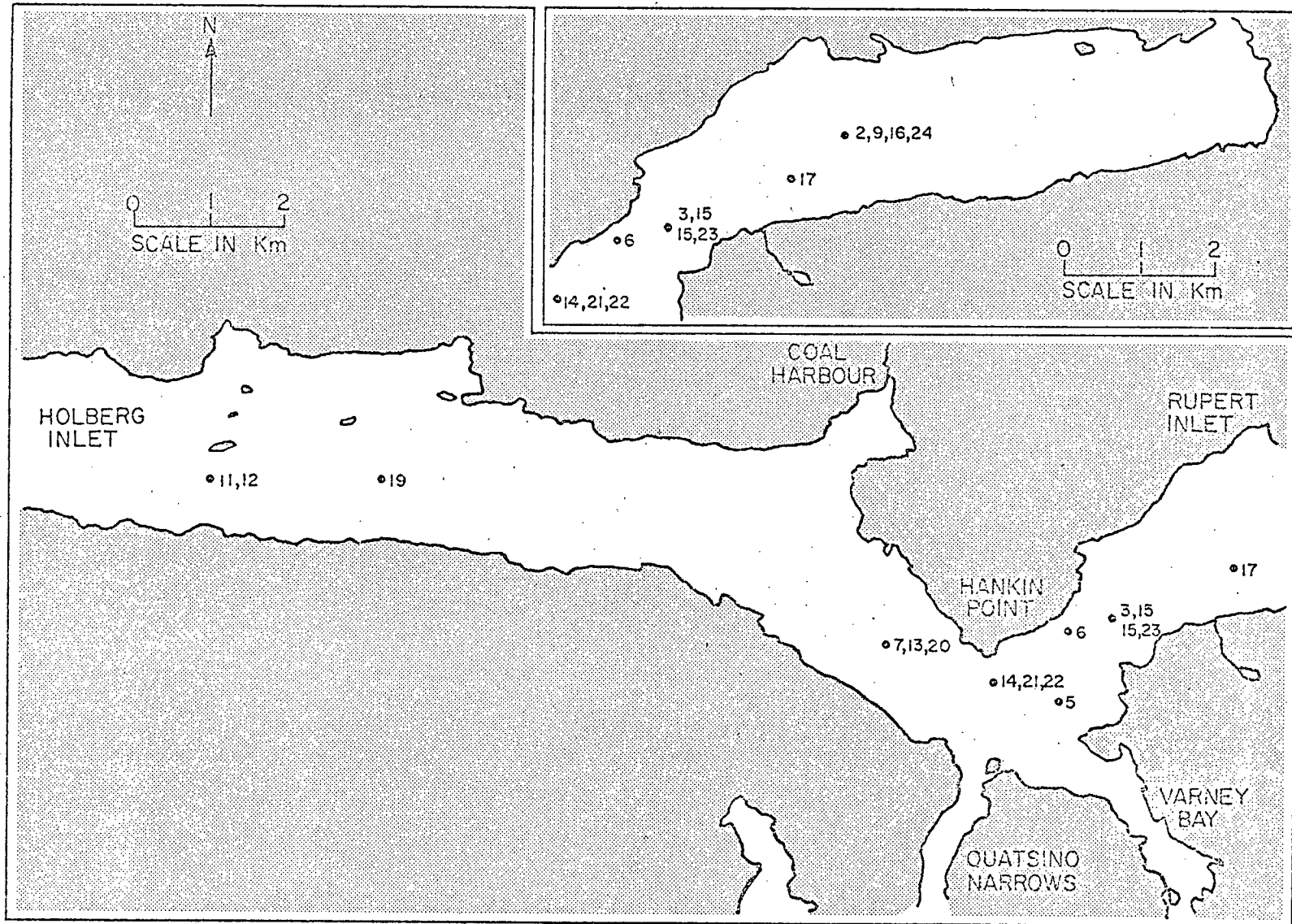


Figure 14: Map showing location of microstructure measurements within Rupert and Holberg Inlets

HEIGHT ABOVE LOW
WATER MARK (metres)

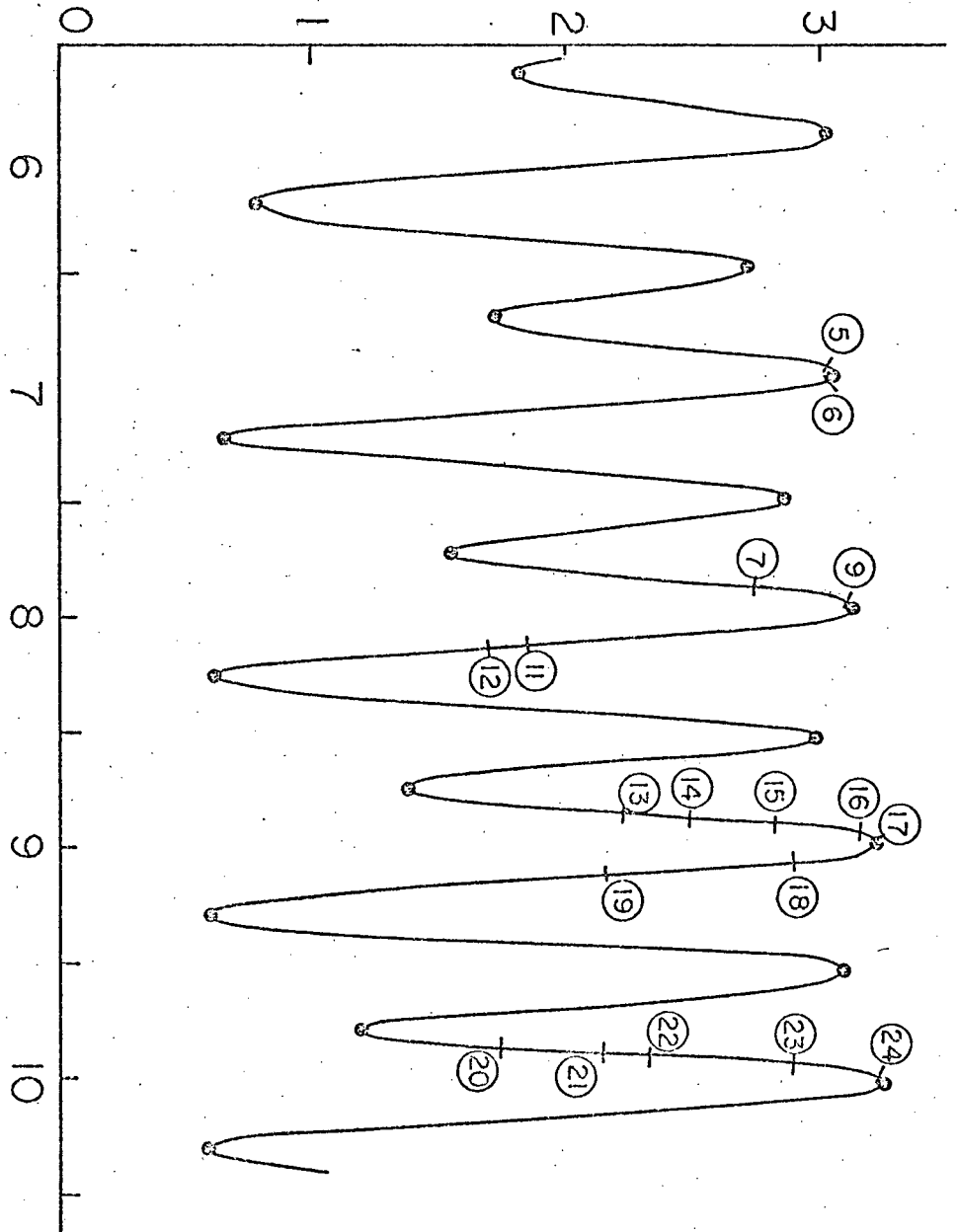


Figure 15: Tidal record at Coal Harbour on Holberg Inlet showing the time at which the microstructure measurements were taken.

Due to the irregular topography, those features observed within the Rupert-Holberg Basin may not be typical of British Columbia Inlets but subsequent measurements in other inlets have produced comparable results. The final section of this chapter contains the information revealed by the micro-structure about the Rupert-Holberg System.

V.2 General Discussion of Thermal Microstructure

Distinction between mixing and stirring in the oceans and atmosphere was first made by Eckart (1948). Velocity differences within a fluid initially cause a steepening of any existing gradients of temperature or concentration and an extension of the interfacial area. This process is called stirring. Mixing is the reduction of these gradients in temperature or concentration by molecular diffusion. The molecular flux is dependent only upon the steepness of the gradient and the coefficients of molecular diffusivity, thus by increasing the gradients stirring serves to hasten mixing. In addition to thereby increasing the flux, stirring increases the amount of mixing by enlarging the area over which mixing takes place. Turbulence is a major source of stirring in the ocean. Causes of turbulence below the upper layers are unknown, but shear instability is strongly suspected. Measurements of small scale thermal gradients disclose the location and the extent of stirring.

Regions of stirring are indicated by numerous, closely spaced (i.e. high frequency) vertical temperature gradients (Fig. 16). These gradients vary in magnitude and fluctuate about a line of zero gradient. Velocity microstructure measurements by Osborn (personal communication) reveal the existence of velocity fluctuations in regions of high frequency temperature gradients. The steepness and magnitude of the temperature gradients depend on the rate of stirring and the molecular diffusion. Sharp gradients confined to one side of the zero gradient line indicate an interface between two temperature zones (Fig. 17). Heat diffusion operates to thicken these interfaces and causes the gradient to widen. The width of the gradient therefore indicates the time since the formation of the interface (Osborn and Cox, 1971). A wider spread denotes an older interface (Fig. 18).

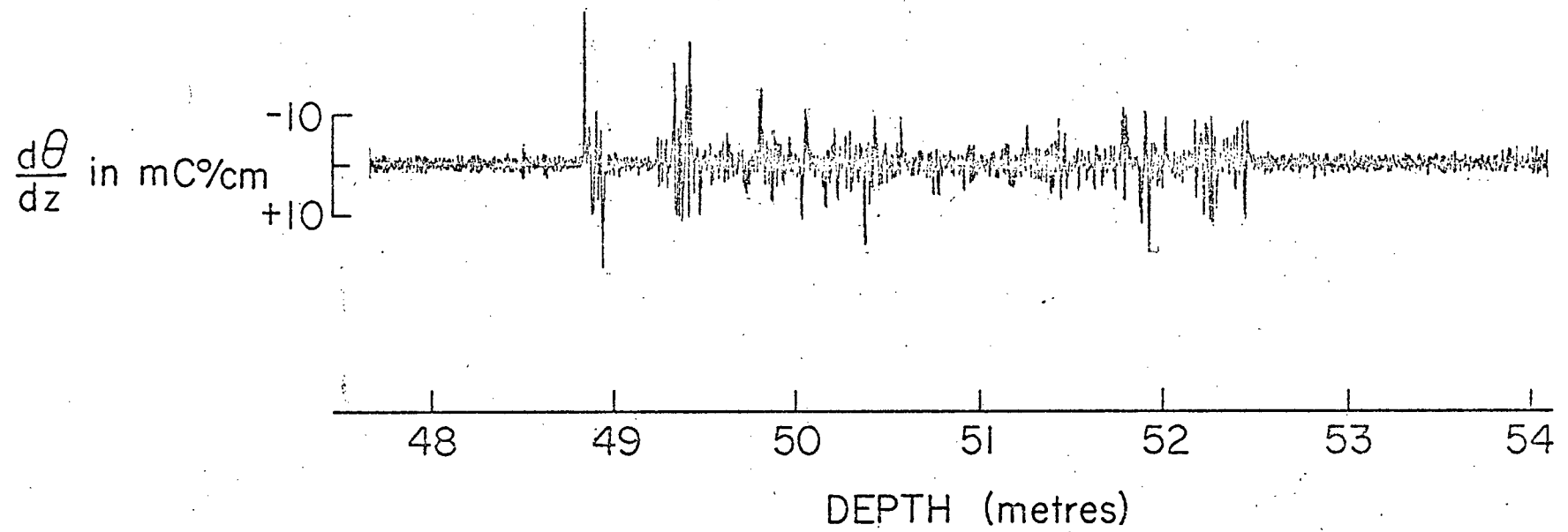


Figure 16: A region of stirring observed during drop number 14.

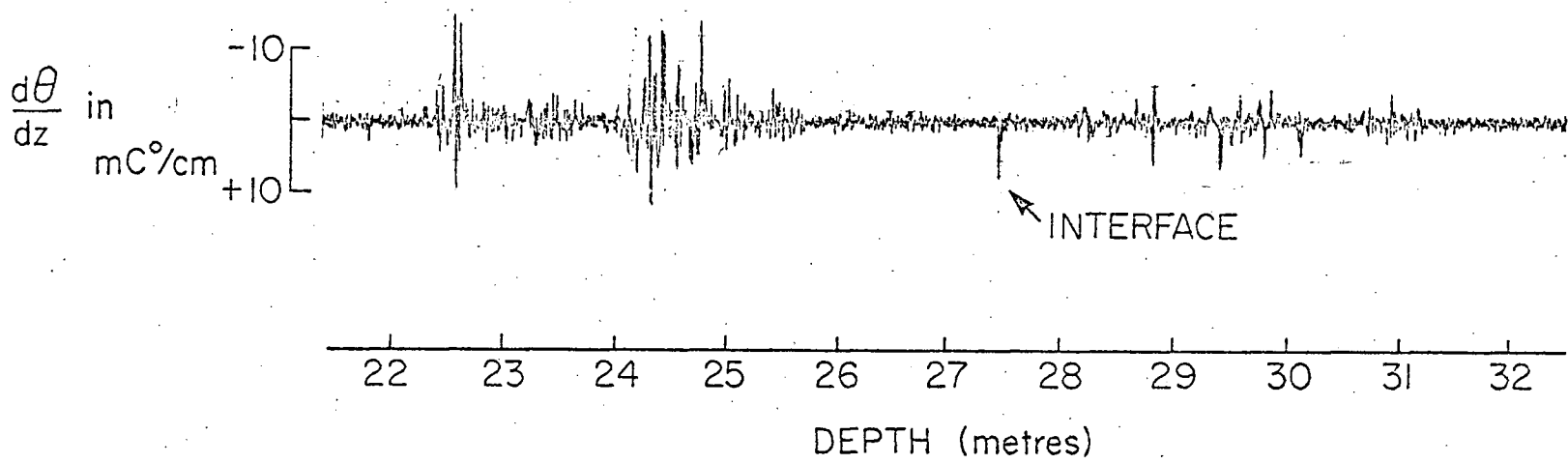
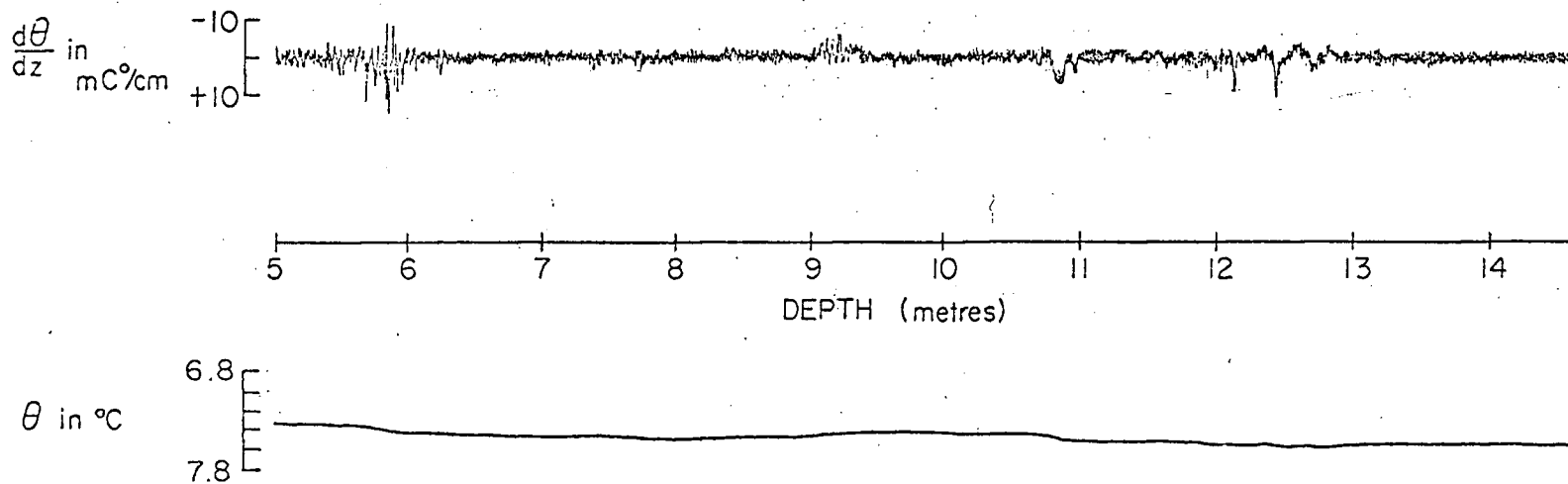


Figure 17: Temperature gradient associated with thermal interface on drop number 21.



* Figure 18: "Older" interfaces observed in Rupert Inlet during drop number 16.

Intrusions are detected by the interjection of warmer or colder water into a homogeneous region (Fig. 19).

The vertical component of the temperature gradient varies considerably throughout the water column. Stirring is normally observed just below the sea surface. Daily variations in the intensity of this stirring suggests control by climatic influences such as wind. Below this zone, irregularly positioned regions of stirrings are detected which vary from tens of centimeters to several meters thick. Sheets and layers as seen by Woods (1970) near Gibraltar are not observed.

Drop number 11 (Fig. 20), taken off Stragglings Islands in Holberg Inlet, illustrates the microstructure associated with the "mixed" layer and the thermocline zone of classical theory. The top 3.5 meters shows an overall temperature spread of only $7.8 \times 10^{-2} \text{ C}^\circ$ but with gradients as high as $3 \times 10^{-2} \text{ C}^\circ \text{ cm}^{-1}$. As mentioned above, the stirring in this layer is most probably due to the "weather". This zone corresponds to the "mixed" layer.

The next seven meters is the thermocline region with the temperature changing by 1.17 C° . This change is concentrated in three interfaces (Fig. 20). Limited stirring occurs below the third interface. The thermocline observed elsewhere in Rupert and Holberg Inlets exhibits stirring throughout the entire region.

The deep region, extending from below the thermocline to the maximum depth attained, usually consists of small temperature changes and limited regions of stirring. On drop number eleven, the temperature spread between 10.5 and 70 meters is approximately 0.2 C° with the gradients seldom reaching beyond the noise level of the instrument. Stirring found within this deep region in most other parts of the inlet is much lower in intensity

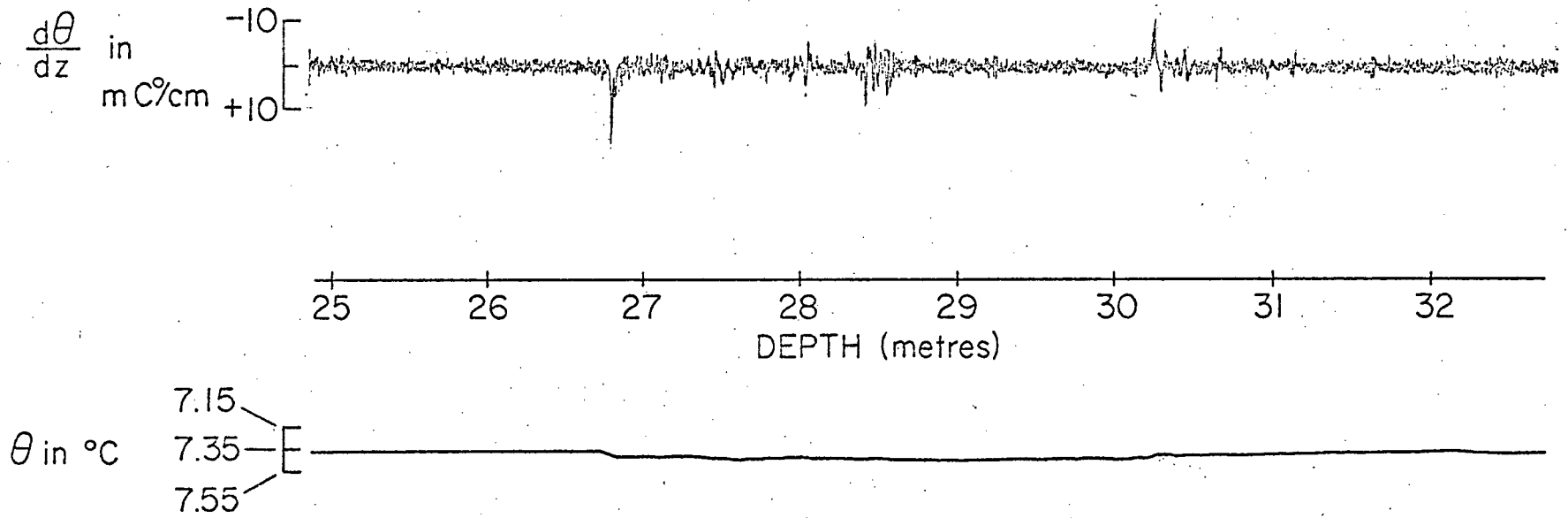


Figure 19: A turbulent intrusion during drop number 23.

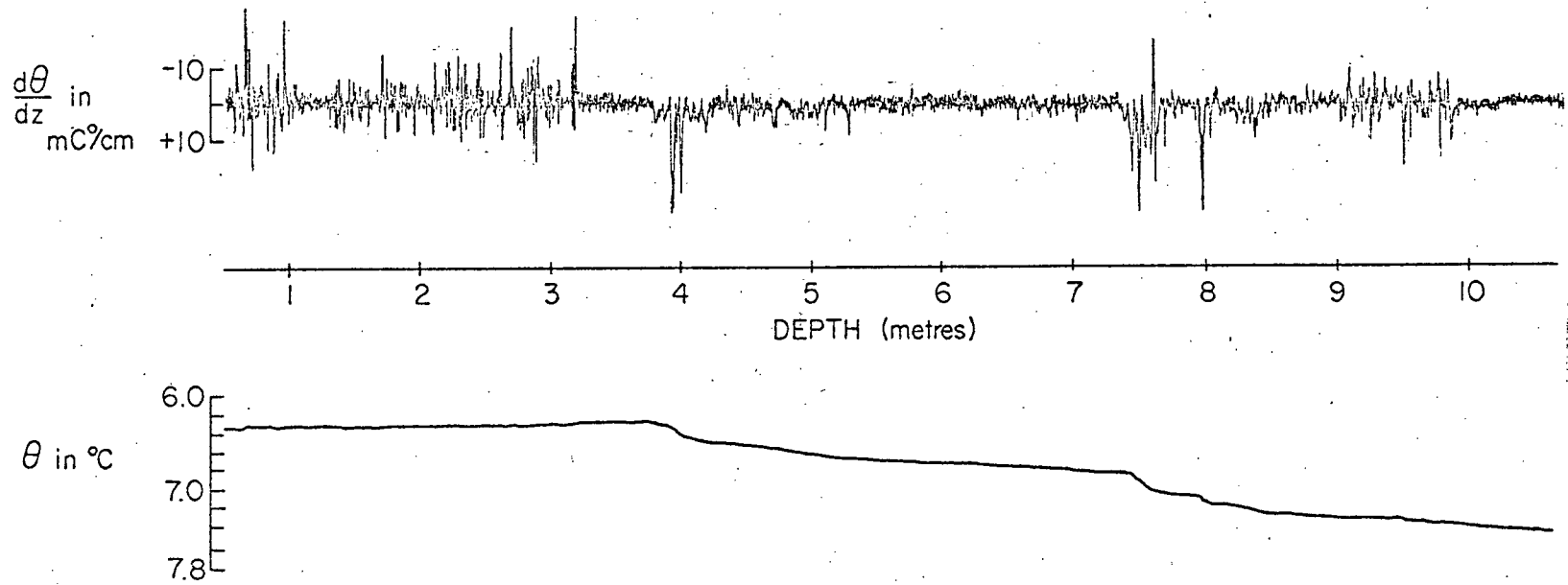


Figure 20: Microstructure associated with the mixed layer and the thermocline in Holberg Inlet.

than the stirring in the upper layers.

A comparison of the temperature gradients recorded by the two thermistors on the instrument shows similarity in large scale properties, such as the positions of regions containing gradients, average magnitudes of the gradients and the existence of large interfaces. Smaller features do not match, lending further support to the idea that these regions are actively stirring. At times one thermistor can be seen to precede the other through a specific gradient by 10 to 30 centimeters (Fig. 21). Calibration of the instrument shows the rocking motion to be too small to produce this difference. However, a required tilt of 30° to the horizontal by the layers presumably causing the gradient seems highly unlikely. This effect has been observed in other inlets with similar instruments but is not always present, (Osborn, personal communication). The reason for this observed difference requires further investigation. The largest difference in structure between the two thermistors occurs during drop number 22 while transecting an intrusion (Fig. 21). The outboard thermistor recorded an intense region of stirring while the central thermistor, one-half meter away, recorded homogeneous conditions. The rotation rate of one ninth of a revolution per second means the outboard thermistor rotated by more than 270 . Cause of this phenomenon is unknown.

V.3 Microstructure in the Rupert-Holberg Basin

Thermal microstructure measurements reveal several important oceanographic characteristics of the Rupert-Holberg system. Opposite Quatsino Narrows, stirring is observed to depths of 98 meters. The size and quantity of stirring in a region just below the thermocline decreases towards

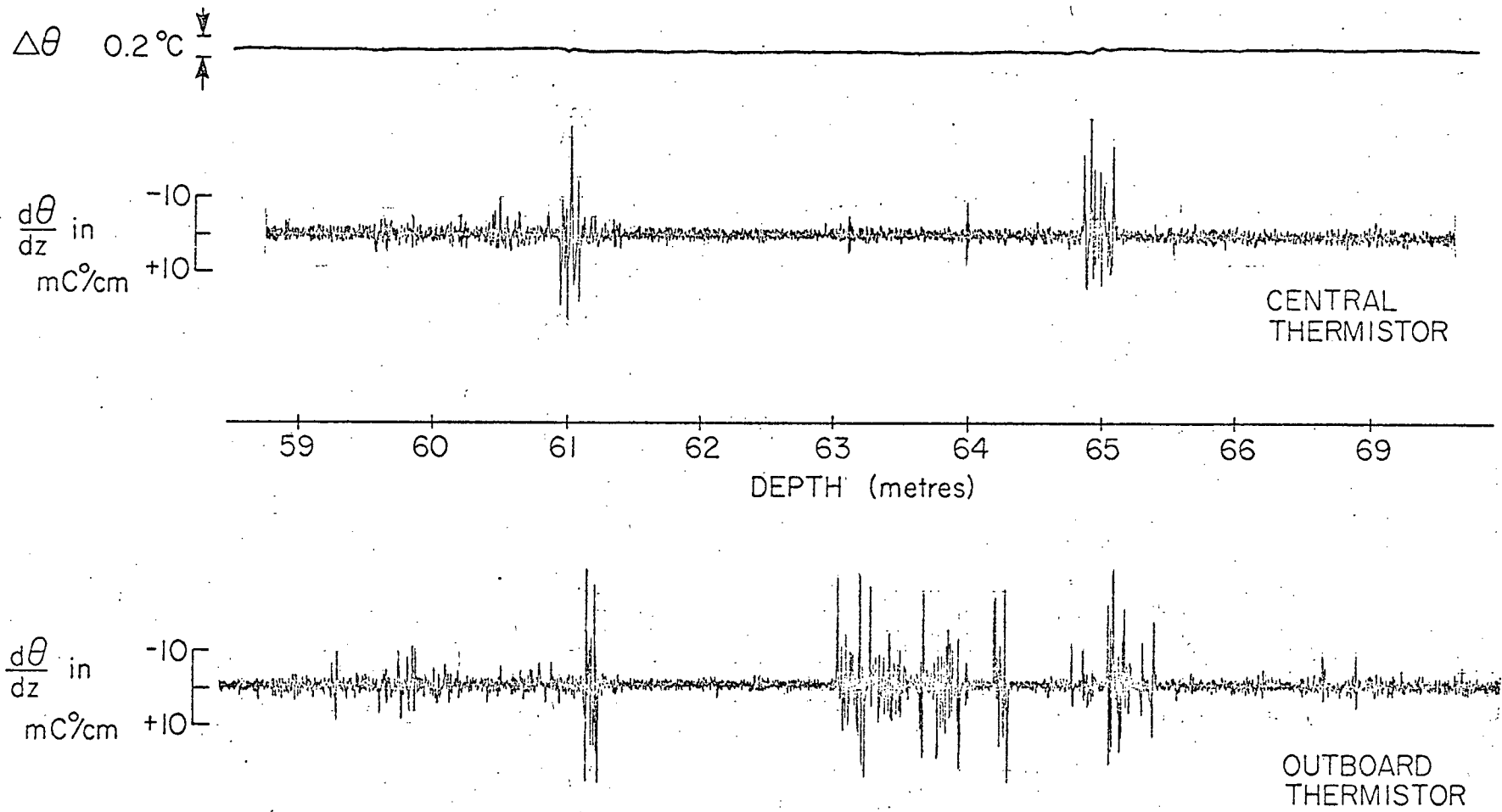


Figure 21: Comparison of the central and outboard thermistors from traces taken during drop number 22.

the head of the inlet. Sporadic stirring of unknown origin is observed below 30 meters, except in the vicinity of the narrows. Of note are the possible daily variations in the relative amounts of stirring between the inlets, although confirmation of this phenomenon requires further investigation.

Measurements taken directly across from Quatsino Narrows towards Hankin Point (drop numbers 14, 21 and 22) reveal numerous stirring regions throughout the water column. Stirring as intense as that usually found only in the upper layers is exhibited between 49 and 53 meters on drop number 14 (Fig. 16), between 43 and 48 meters on drop number 21 and between 84 and 90 meters on drop number 22 (Fig. 22). The maximum depths attained during these drops are 65, 60 and 98 meters respectively. All these drops were taken near times of maximum expected tidal currents in the narrows (Fig. 15). These measurements are in agreement with the predictions of the model as presented in chapter IV. The observed stirring originates from two sources. These are the inherent turbulence of the intruding water and the locally induced stirring caused by these intrusions. Both sources work to mix the water in this part of the inlet. Distinction between these sources of stirring in a particular region cannot be determined with the present instrument. The depth to which stirring occurs during these drops is not surprising upon investigation of the water properties in Quatsino Sound. Bottle casts during the first days of the microstructure measurements reveal the density at 10 meters depth in the sound to be greater than in the top 75 meters of water in the basin. The density at 15 meters in Quatsino Sound is larger than the maximum density found in the basin. Gravitational effects alone seem capable of transporting the upper layers from the sound to the depths of observed stirring

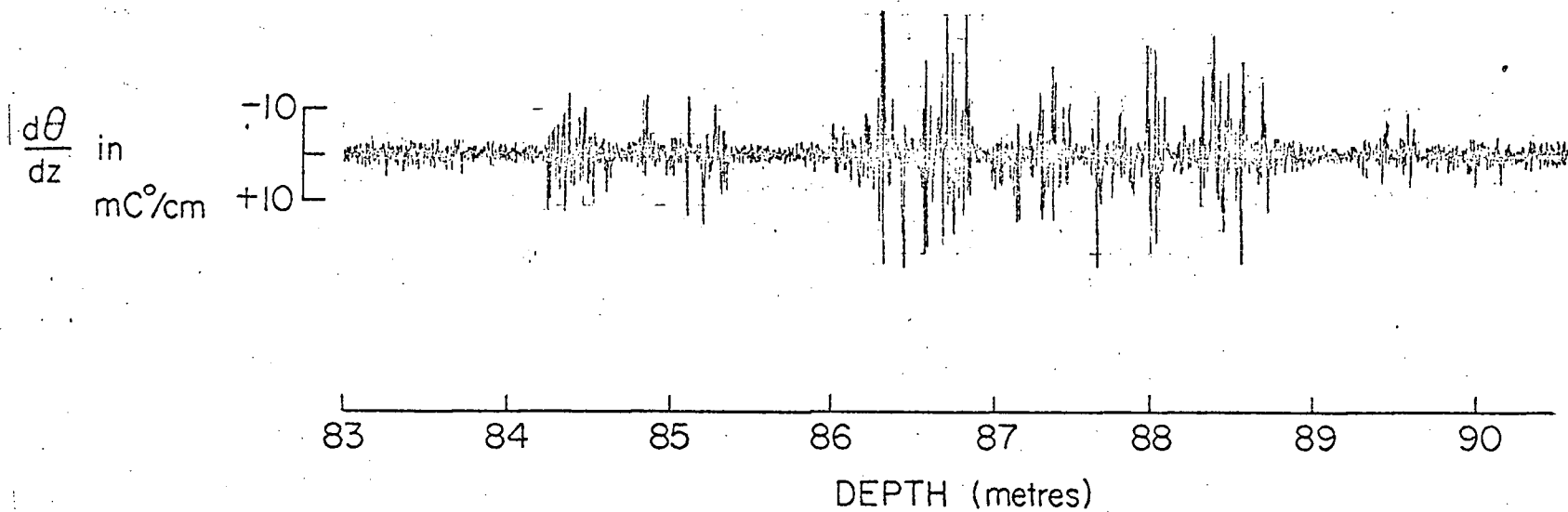


Figure 22: Deep stirring found opposite Quatsino Narrows on drop number 22.

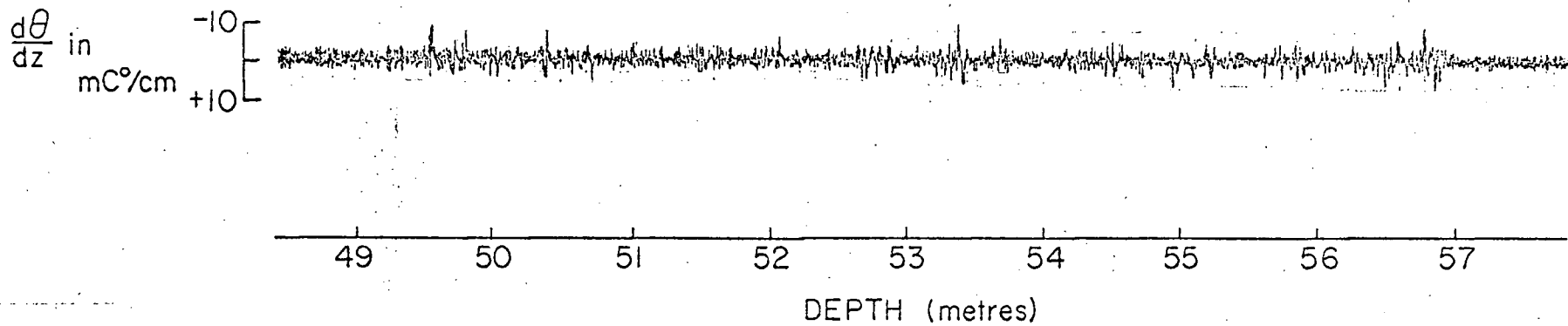


Figure 23: Deep stirring in Rupert Inlet during drop number 18.

following passage through Quatsino Narrows. The pushing aside of the upper layers by the incoming tide is directly observed during drop number 14. No thermocline exists as the temperature increases by less than 0.3°C over the entire depth.

The measurements taken at the entrance to Holberg Inlet (drop numbers 7, 13 and 20) all reveal stirring between the bottom of the thermocline (at 7 meters) and approximately 30 meters. This zone contains the warmest water within the water column. The three drops (numbers 11, 12 and 19) taken near the Stragglings Islands all show a warm zone between the bottom of the thermocline (10 meters) and 28 meters. Stirring occurs only near the bottom of this zone, with the temperature gradients of its interior implying small but stable interfaces. The magnitude of the temperature gradients decreases from the narrows towards the head. Across from Quatsino Narrows, gradients of $50 \times 10^{-3} \text{ }^{\circ}\text{C}/\text{cm}$. are not uncommon while at the entrance to Holberg they decrease to $20 \times 10^{-3} \text{ }^{\circ}\text{C}/\text{cm}$. and by Stragglings Islands diminish to between $5-10 \times 10^{-3} \text{ }^{\circ}\text{C}/\text{cm}$. The quantity of stirring also decreases in an up inlet direction. These features can be explained by a flow up Holberg Inlet, originating from the vicinity of Quatsino Narrows and reaching beyond Stragglings Islands. Generation of such a flow is expected (see section IV.2). The warm layer in which the flow is found may have arisen through localized warming and subsequent cooling of the surface layer or may possibly be the remainder of an earlier warm water intrusion originating from Quatsino Sound. The bottle stations reveal the intruding tidal water to be colder than this warm zone. Hence as expected the maximum observed temperature increases towards the head of the inlet. Occasional stirring below this zone is also detected, the largest region being between 48 and 55 meters during drop number 20.

Conditions within Rupert Inlet suggest an up-inlet flow under the thermocline, reaching half way up the inlet. The magnitude and amount of visible stirring decreases towards the head of the inlet. A warm zone between the bottom of the thermocline (at 5 to 10 meters) and 30 meters exists in Rupert. Arguments, similar to those produced for Holberg Inlet, suggest a relationship between this current and the tides. As in Holberg, the furthest up inlet measurements reveal stable interfaces below the thermocline (Fig. 18). Deep stirring occurs within Rupert on an infrequent basis. It is most evident during drop number 18 (Fig. 23) between 49 and 57 meters where magnitudes of the gradients are as high as any below the thermocline. Also a section between 80 and 90 meters on this drop shows signs of stirring. A 2 meter region of stirring centered at 57 meters is seen during drop number 24.

The amount of stirring at one station varies hourly as well as daily. On March 9, drops number 15 and 18 were taken on a flood and ebb tide respectively with the latter showing more evidence of stirring. This day is not as active as March 10 (drop 23) during a flood tide nor March 6 (drop 3) near low water slack. Winds of 2 to 8 knots from varying directions during March 9 compare with winds of 10 to 20 knots blowing generally up Rupert Inlet during the other two days. This may indicate a correlation between speed and direction of wind and the amount of stirring.

The relative amounts of stirring between Rupert and Holberg appear to change daily. More stirring occurs up Holberg Inlet on March 8, equal stirring occurs on March 9 and more stirring occurs up Rupert on March 10. The days prior to March 8 do not contain enough data to determine a preference. Due to the hourly variations at each station more data are needed

to actually confirm that changes in the relative amounts of stirring do occur.

CHAPTER VI

COMPARISON WITH OTHER SHALLOW SILLED INLETS

Mixing within an inlet is revealed by near uniform conditions of temperature and salinity plus high oxygen values. The mixing may be continual in nature or caused by a recent flushing of the inlet. Lack of uniform conditions or the existence of low oxygen values eliminates the possibility of a continuous mixing process. Data collected by the University of British Columbia since 1951 is examined to determine the mixing characteristics of inlets with a similar geographical configuration to the Rupert-Holberg basin. Establishment of the essential factors necessary for continual mixing are sought.

This investigation is restricted to British Columbia inlets listed by Pickard (1961, 1963) whose sill depths are less than 30 meters. Also, only those inlets connected by a long, narrow channel are considered.

Indian Arm, Sechelt, Belize, Seymour Inlets and Work Channel all possess the necessary geographic features. They do however exhibit non-uniform water properties. Indian Arm and Work Channel show a more gradual increase in depth away from the sill than is found in the Rupert-Holbert basin. This may explain the absence of thorough mixing within these inlets. In Sechelt, Belize and Seymour Inlets, the ratio of the tidal prism to the total volume is less than one to one hundred. Such small tidal flow would produce correspondingly small effects on the water properties.

Drury Inlet and Porcher Inlet both display near uniform water properties. Only one survey has been conducted in each inlet, therefore further data are required to determine if tidally induced vertical mixing does occur on a regular basis.

Uniform conditions of temperatures, salinity and oxygen exist below 20 meters depth in Fortune Channel, between Bedwell Sound and Tofino Inlet on Vancouver Island (Fig. 24). Coote (1964) attributes these conditions to tidal action. A sill of 28 meters in Matlset Narrows, which separates Fortune Channel from Bedwell Sound, causes tidal currents of 3 - 4 knots. The maximum depth in Fortune Channel is 140 meters and lies just beyond the sill. Of possible importance is the shore directly opposite the narrows as the basin lies perpendicular to the narrows. This shoreline may act to force the oncoming tidal waters into the deeper sections of the basin. Rupert-Holberg also contains a shore opposite its narrows. This factor may play a significant role in the mixing process. The major fresh water inflow for Fortune Channel originates from the Kennedy River which enters half way up Tofino Inlet and flows through Dawley Pass. Thus a much less saline upper layer exists in Fortune Channel than in Rupert Inlet.

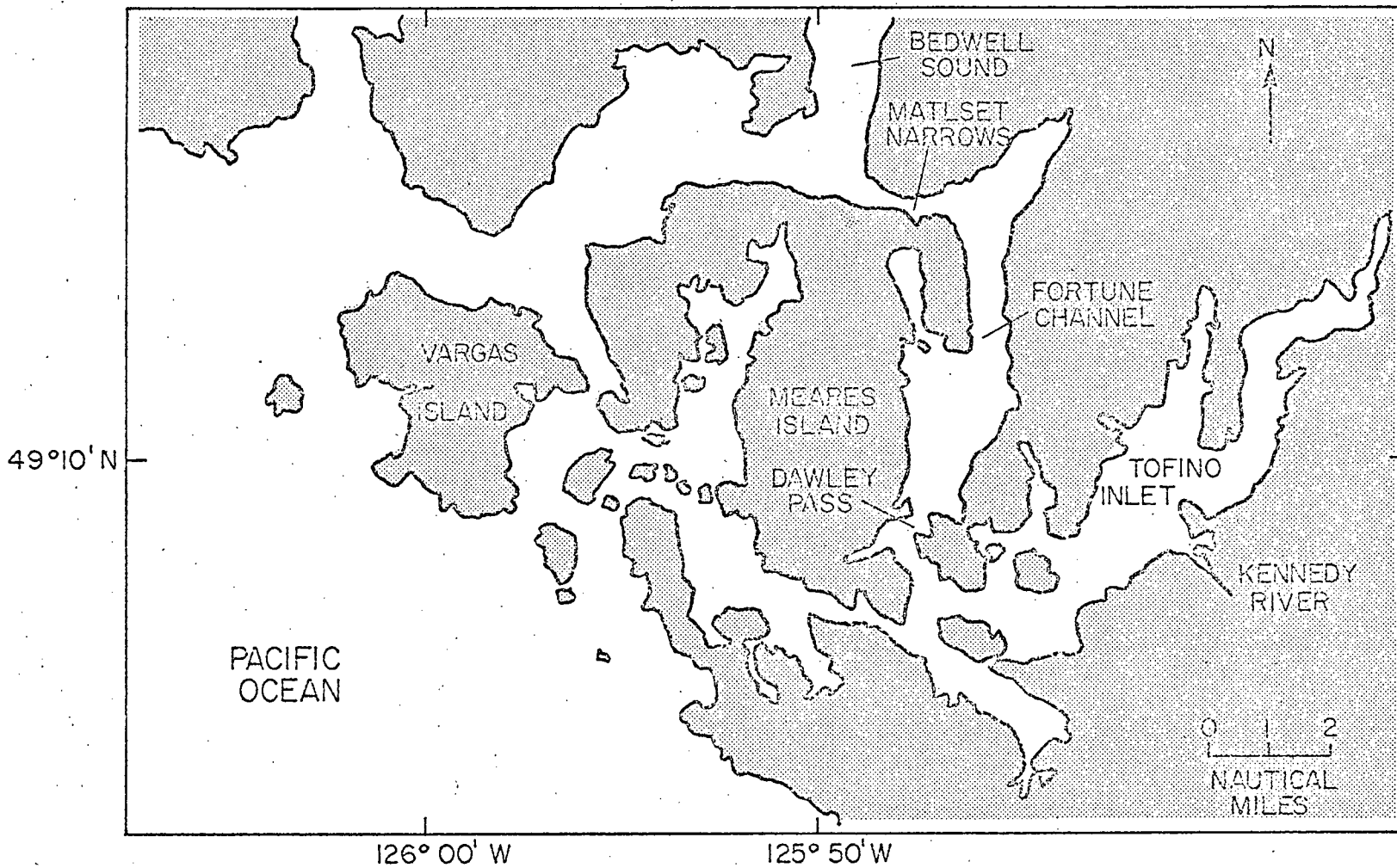


Figure 24: Map of Fortune Channel and surrounding area.

CHAPTER VII

CONCLUSION

The study of the Rupert-Holberg system reveals a well mixed water body which experiences large monthly variations in density. Two processes account for these observations. Decreases in density are due to mixing lower salinity water into the basin. Vigorous stirring, caused by tidal action, mixes the water just beyond the narrows. This stirring is enhanced by the flow of the turbulent tidal intrusions beneath the existing low salinity layer. Energy for this process derives from the tide. The depth and degree of mixing changes with each tidal cycle. Increases are caused by gravitational flow of dense water over the sill and onto the basin floor. Both processes contribute to high oxygen values in the basin. Continuous mixing exists due to one or other of these processes. Internal mixing within the rest of the basin is presumed to proceed by pressure gradient currents. Further investigation is required to determine a detailed picture of the mixing away from the narrows. A study to reveal the time response of the inlet to changes in river discharge is also suggested.

Thermal microstructure measurements reveal stirring in the vicinity of the narrows and the existence of an up inlet flow in both Rupert and Holbert Inlets. Studies within the inlets which combine the use of large and small scale measurements will greatly extend the existing knowledge of these areas. This seems even more likely with the newly developed instruments which measure velocity, salinity and temperature microstructure, simultaneously.

Comparison with British Columbia inlets of similar topography reveals

only Fortune Channel on Vancouver Island to exhibit like mixing conditions. This suggests that a shoreline opposite the narrows may be important to deflect oncoming tidal water into the basin. Porcher and Drury Inlets show signs of similar mixing properties, however confirmation requires further data.

A classification of all inlets as to their mixing properties would be highly advantageous. It would assist in locating future industries planning to deposit wastes in inlets. Depending upon the type of disposal system required, such as high oxygen demand, dilution, etc., the most suitable inlet could be chosen. If an industry is required to be located on a specific inlet, knowledge of the mixing properties of that inlet would help to determine where the waste disposal system should be located.

REFERENCES

- Canadian Hydrographic Service, 1971. Canadian Tide and Current Tables. Volume 6. Queen's Printer. 75 pp.
- Canadian Hydrographic Service, 1972. Tidal Currents, Quatsino Narrows, British Columbia Queen's Printer, Ottaws, 10 pp.
- Coote, A.R. 1964. A Physical and Chemical Study of Tofino Inlet, Vancouver Island, British Columbia. M.Sc. Thesis University of British Columbia, Vancouver, B.C.
- Eckart, Carl. 1948. An Analysis of the Stirring and Mixing Processes in Incompressible Fluids. Journal of Marine Research, 7, 265-275.
- Lane, R.K. 1962. A Review of Temperature and Salinity Structures in the Approaches to Vancouver Island, British Columbia. Journal of Fisheries Board of Canada, 19, 45 - 91.
- Osborn, T. R. 1973. Vertical Profiling of Velocity Microstructure. (In Progress)
- Osborn, T. R. and Cox, C.S. 1972. Oceanic Fine Structure, Geophysical Fluid Dynamics, 3, 321-345.
- Pickard, G.L. 1956. Physical Features of British Columbia Inlets. Transactions of the Royal Society of Canada, Series III, 50, 47 - 58.
- Pickard, G. L. 1961. Oceanographic Features of Inlets in the British Columbia Coast. Journal of Fisheries Research Board of Canada, 18, 907 - 999.
- Pickard, G. L. 1963. Oceanographic Characteristics of Inlets of Vancouver Island, British Columbia. Journal of Fisheries Research Board of Canada, 20, 1109 - 1144.
- Strickland, J.D.H. and Parsons, T. R. 1968. A Practical Handbook of Seawater Analysis Queen's Printer, Ottawa, 311 pp.

- Taylor, G. I. 1919. Tidal Friction in the Irish Sea. Philosophical Transactions of the Royal Society (A), 220, 1 - 33.
- Tully, J. P. 1949. Oceanography and Prediction of Pulp Mill Pollution in Alberni Inlet. Fisheries Research Board of Canada, Bulletin No. 83, 169 pp.
- Waldichuk, M. 1958. Some Oceanographic Characteristics of a Polluted Inlet in British Columbia. Journal of Marine Research, 17, 536 - 551.
- Waldichuk, M., Markert, J.R., and Meikle, J.H. 1968. Physical and Chemical Oceanographic Data from From the West Coast of Vancouver Island and the Northern British Columbia Coast, 1957 - 1967. Fisheries Research Board of Canada, Manuscript Report Series No. 990, 161 pp.
- Woods, J. W. 1968. Wave-Induced Shear Instability in the Summer Thermocline. Journal of Fluid Mechanics, 32, 791 - 800.